

A revised inoceramid biozonation for the Upper Cretaceous based on high-resolution carbon isotope stratigraphy in northwestern Hokkaido, Japan

TATSUYA HAYAKAWA¹ AND HIROMICHI HIRANO²

¹*Department of Earth Sciences, Resources and Environmental Engineering, Graduate School of Creative Science and Engineering, Waseda University, Nishi-waseda 1-6-1, Shinjuku-ku, Tokyo 169-8050, Japan, Present address: TS Network Co., Ltd., Asakusabashi 4-17-7, Taito-ku, Tokyo 111-0053, Japan.*

E-mail: hanamizuki@y.asagi.waseda.jp

²*Department of Earth Sciences, School of Education, Waseda University, Nishi-waseda 1-6-1, Shinjuku-ku, Tokyo 169-8050, Japan. E-mail: hhirano@waseda.jp*

ABSTRACT:

Hayakawa, T., Hirano, H. 2013. A revised inoceramid biozonation for the Upper Cretaceous based on high-resolution carbon isotope stratigraphy in northwestern Hokkaido, Japan. *Acta Geologica Polonica*, **63** (2), 239–263. Warszawa.

Biostratigraphic correlations of inoceramid bivalves between the North Pacific and Euramerican provinces have been difficult because the inoceramid biostratigraphy of the Japanese strata has been based on endemic species of the north-west Pacific. In this study, carbon stable isotope fluctuations of terrestrial organic matter are assembled for the Upper Cretaceous Yezo Group in the Haboro and Obira areas, Hokkaido, Japan, in order to revise the chronology of the inoceramid biozonation in Japan. The carbon isotope curves are correlated with those of marine carbonates in English and German sections with the aid of age-diagnostic taxa. According to the correlations of the carbon isotope curves, 11 isotope events are recognised in the sections studied. As a result of these correlations, the chronology of the inoceramid biozones of the Northwest Pacific has been considerably revised. The revised inoceramid biozones suggest that the timing of the origination and extinction of the inoceramids in the North Pacific biotic province is different from the stage/substage boundaries defined by inoceramids, as used in Europe and North America.

Key words: Carbon isotope stratigraphy; Inoceramid biozones; Yezo Group; Upper Cretaceous; Hokkaido; Japan.

INTRODUCTION

Inoceramid bivalves show a high taxonomic diversity in the Upper Cretaceous, and are important age-diagnostic forms in global correlations (e.g., Ogg *et al.* 2004). Inoceramids are also abundant in the Cretaceous strata exposed in Hokkaido, Japan (e.g., Takahashi 2005), and inoceramid-based biostratigraphic studies have been carried out for a long time (e.g., Matsumoto 1959; Tanabe *et al.* 1977). Toshimitsu *et al.* (1995) inte-

grated the ammonoid, inoceramid, foraminiferal, radiolarian and palaeomagnetic stratigraphies, and their scheme is widely followed in biostratigraphic studies in Japan (e.g., Wani and Hirano 2000; Moriya and Hirano 2001; Oizumi *et al.* 2005). Unfortunately, the North Pacific biotic province was well established since the Middle Albian (Iba and Sano 2007) and only a few inter-provincial age-diagnostic taxa are known from the Japanese Upper Cretaceous, such as *Mytiloides incertus* (Jimbo), also reported from the Upper Turonian of the

Euramerican and South African provinces (e.g., Tröger 1967; Noda 1984; Noda and Matsumoto 1998; Walaszczyk and Cobban 2000; Diebold *et al.* 2010). The Japanese ammonoid zonation and interprovincial correlations using ammonoids were established by Matsumoto (e.g., Matsumoto 1959; Matsumoto 1977), and have subsequently been applied by later workers to the Japanese inoceramid successions. Age-diagnostic ammonoids, however, are rare; whereas inoceramids are more common. Consequently, establishing the reliable chronostratigraphic ranges of critical inoceramid taxa is of the utmost importance in correlation of the Japanese succession with the international standard zonal scheme.

Following the pioneering work of Scholle and Arthur (1980), carbon stable isotope studies are used to provide an effective chronostratigraphic framework. Temporal fluctuations in the carbon isotope ratios ($\delta^{13}\text{C}$) of marine carbonates are a reliable tool for regional and international correlations (e.g., Jenkyns *et al.* 1994; Erbacher *et al.* 1996; Voigt and Hilbrecht 1997; Stoll and Schrag 2000; Voigt 2000; Jarvis *et al.* 2002, 2006; Voigt *et al.* 2010). In Japan, $\delta^{13}\text{C}$ stratigraphic studies on terrestrial organic matter have been undertaken for the Yezo Group (Hasegawa 1992; Hasegawa and Saito 1993; Hasegawa 1997; Hirano and Fukuju 1997; Hasegawa and Hatsugai 2000; Ando *et al.* 2002, 2003; Hasegawa *et al.* 2003; Ando and Kakegawa 2007; Uramoto *et al.* 2007, 2009; Takashima *et al.* 2010). Hasegawa (1997) discussed the resemblance between the $\delta^{13}\text{C}$ curves for marine carbonates and those for terrestrial organic matter, and concluded that the $\delta^{13}\text{C}$ stratigraphy of terrestrial organic matter provides a reliable tool for correlation with the marine carbonates. Recently, Uramoto *et al.* (2009) supported the usefulness of this tool for correlation and indicated that $\delta^{13}\text{C}$ fluctuations of terrestrial organic matter reflected the global isotopic patterns in the carbon reservoir of the ocean-atmosphere-terrestrial biosphere system. The $\delta^{13}\text{C}$ -based correlations first require, however, determination of the approximate geological ages, based usually on biostratigraphy and complete stratigraphic successions.

The purpose of this study is to revise the chronostratigraphic position of the inoceramid biozones in Japan based on $\delta^{13}\text{C}$ correlations between Japan and Europe. Although Uramoto *et al.* (2009) demonstrated the $\delta^{13}\text{C}$ stratigraphy in the Obira area, the sampling intervals for the Coniacian were rather coarse, and their $\delta^{13}\text{C}$ record was limited to the Santonian. In the present study, higher-resolution $\delta^{13}\text{C}$ data are reported, and the analysis spans the Coniacian through to the lower Campanian. The need for a chronostratigraphic revision of the Japanese inoceramid zonation was indicated by Takashima *et al.* (2010) in their high-resolution $\delta^{13}\text{C}$ stratigraphy for the Upper Cenomanian through to Lower Campanian of

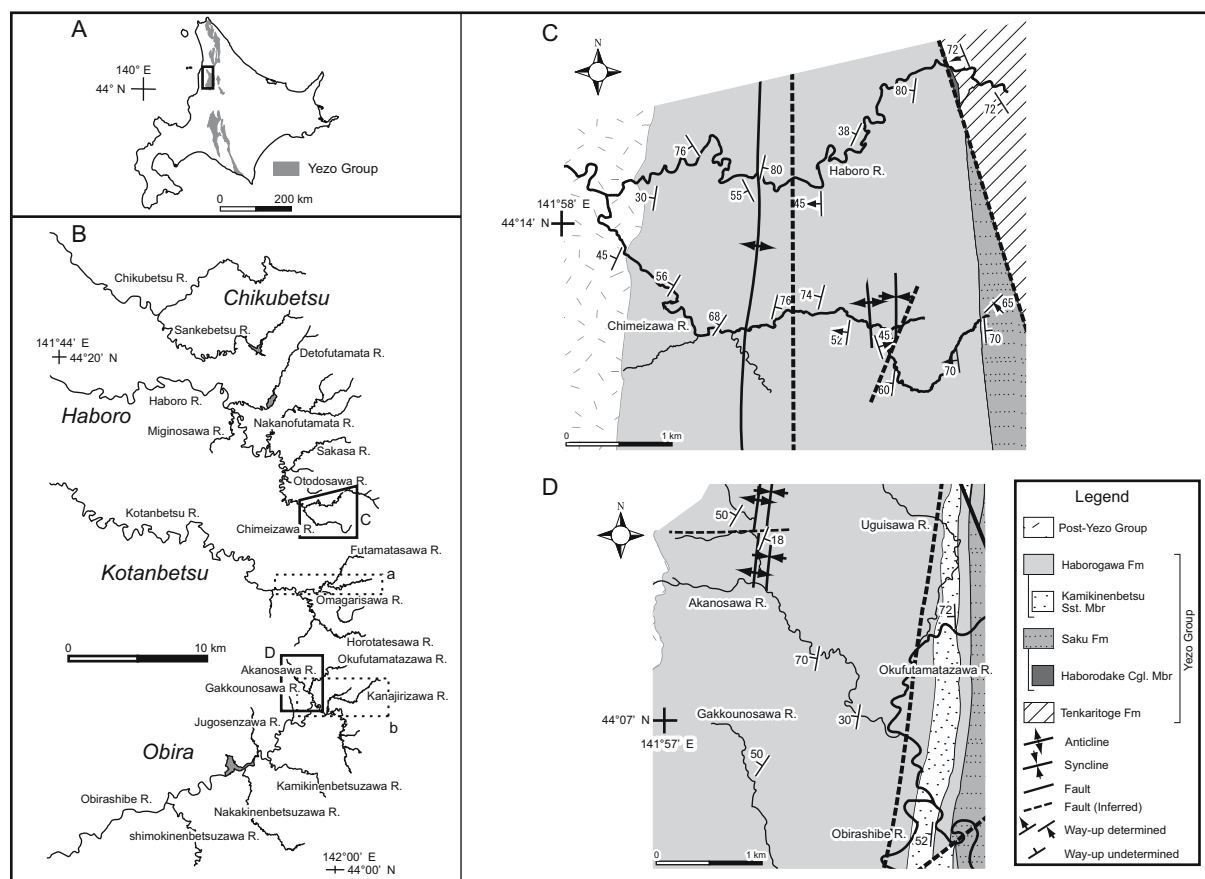
the Kotanbetsu area of Hokkaido. However, Takashima *et al.* (2010) reported the $\delta^{13}\text{C}$ data from a single area and the only fossil records used were those of the inoceramids reported by Wani and Hirano (2000) from the same section. In the present study, on the other hand, the $\delta^{13}\text{C}$ analyses were performed on material from sections with rich macrofossil and microfossil records in two different areas of Hokkaido. The high-resolution $\delta^{13}\text{C}$ stratigraphy from the upper Turonian to the lower Campanian of the studied succession was then compared with the $\delta^{13}\text{C}$ fluctuations reported by Voigt and Hilbrecht (1997), Hasegawa *et al.* (2003), Jarvis *et al.* (2006), Takashima *et al.* (2010), and Voigt *et al.* (2010).

GEOLOGICAL SETTING

The Yezo Group is interpreted as forearc basin sediments (Okada 1982), which consist of hemipelagic and shallow marine mudstone and sandstone (e.g., Ando 2003; Takashima *et al.* 2004) with abundant molluscan fossils.

The studies were carried out in the Haboro and Obira areas (Text-fig. 1). The middle to upper parts of the Yezo Group crop out in both areas and yield abundant macrofossils. The Yezo Group is overlain unconformably by the Eocene Sankebetsu Formation (lower part) in the Haboro area and by the Miocene Jugosenzawa Formation in the Obira area. The lithostratigraphy in both areas was discussed by Igi *et al.* (1958), Tsushima *et al.* (1958), Tanaka (1963), Yamaguchi and Matsuno (1963), Toshimitsu (1985, 1988), Okamoto *et al.* (2003), Funaki and Hirano (2004), Takashima *et al.* (2004), and Oizumi *et al.* (2005). The Yezo Group has been subdivided into many lithostratigraphic units in northern Hokkaido (Igi *et al.* 1958; Tanaka 1963; Tanabe *et al.* 1977). Subsequently, some authors followed these lithostratigraphic units in the Haboro area (Okamoto *et al.* 2003) and the Obira area (Funaki and Hirano 2004; Oizumi *et al.* 2005). The lithostratigraphic classification of Funaki and Hirano (2004) and Oizumi *et al.* (2005) is followed herein.

In the sections studied, the Yezo Group is subdivided into the Saku Formation and the conformably overlying Haborogawa Formation. The Saku Formation is built of alternating sandstone and siltstone. The Haborogawa Formation is represented mainly by bioturbated dark grey mudstone with some coarsening-upward sequences that characterise the middle and upper parts of the formation. In the Obira area, a fine- to coarse-grained sandstone with slump deposits is developed in the lowest part of the Haborogawa Formation, and is a good regional key marker-bed (Kamikinenbetsu Sandstone Member; Funaki and Hirano 2004).



Text-fig. 1. (A) Map showing the distribution of the Yezo Group. The rectangle contains the study areas. (B) The study areas. The northern rectangle is the Haboro area, the southern area is the Obira area, the middle rectangle with dashed line (a) is the Kotanbetsu area studied by Takashima *et al.* (2010), and the southern rectangle with dashed line (b) is the area studied by Uramoto *et al.* (2007, 2009). (C) Geological map of the Haboro area. (D) Geological map of the Obira area in Hokkaido, Japan.

The geological map in the Obira area is modified after Funaki and Hirano (2004) and Oizumi *et al.* (2005)

The Saku and Haborogawa formations have yielded well-preserved and abundant macro- and microfossils (Tanaka 1963; Tanabe *et al.* 1977; Sekine *et al.* 1985; Toshimitsu 1985, 1988, Toshimitsu *et al.* 1998; Okamoto *et al.* 2003; Funaki and Hirano 2004; Oizumi *et al.* 2005). The upper Turonian through to lower Campanian is documented.

MATERIALS AND METHODS

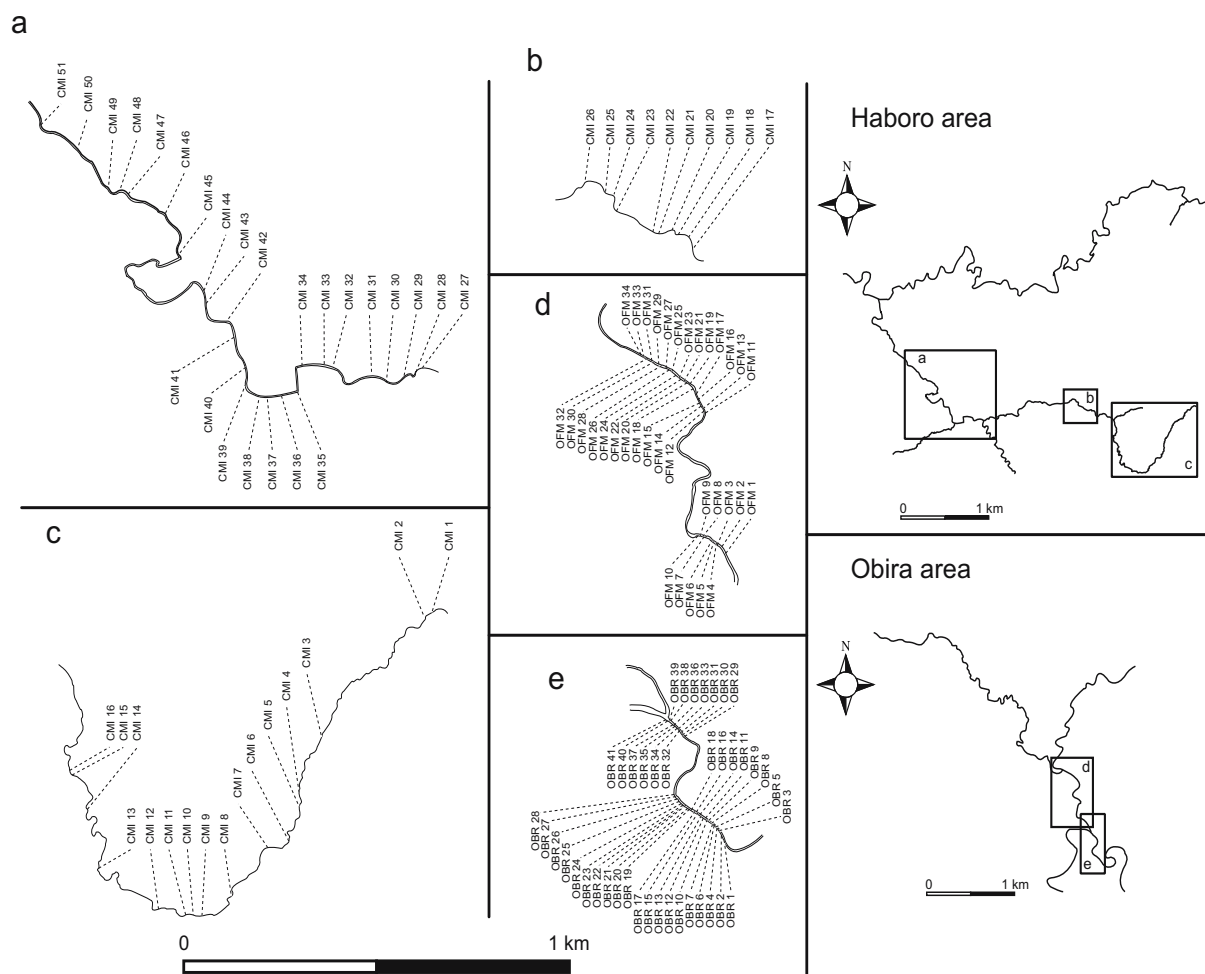
In this study, 123 mudstone and sandy mudstone samples were collected along the Chimeizawa River in the Haboro area (48 samples) and along the Obirashibe and Okufutamatazawa Rivers in the Obira area (75 samples) (Text-fig. 2).

To evaluate the kerogen type and the maturity of the organic matter, the total organic carbon (TOC) contents and Rock-Eval pyrolysis were analysed.

Powdered mudstone samples were treated with 6N

HCl for 24 hours to remove carbonates. The elemental composition of 20–30 mg of each sample was analysed using a J-SCIENCE LAB Co., Ltd. Micro Corder JM10, calibrated with antipyrine ($C_{11}H_{12}N_2O$) as the standard. The elemental composition of each sample was corrected based on the weight-percent of removed carbonates, and the TOC content of the whole rock was obtained.

The Rock-Eval pyrolysis was conducted using a VINCI Technologies model 6 device. The 100 mg powdered samples were pyrolysed from 300 to 650°C with a rate of heating of 25°C/min in a nitrogen atmosphere. The S1 is the amount of hydrocarbon that can be thermally distilled and was analysed with a flame ionisation detector (FID). The S2 is the hydrocarbons released by pyrolytic degradation of the kerogen and was analysed with the FID. The S3 is the carbon dioxide generated during pyrolysis at 390°C and was analysed with thermal conductivity detection (TCD). The temperature at which the maximum amount of S2 hydrocarbons was generated is T_{max} . The Hydrogen Index (HI) is the ra-



Text-fig. 2. Map showing the locations of the mudstone samples in the Haboro and Obira areas

tio of mg HC in S2/g TOC. The Oxygen Index (OI) is the ratio of mg CO₂ in S3/g TOC.

For the $\delta^{13}\text{C}$ analysis, the acid-processed samples were treated with a mixture of dimethyl ether and methanol (93:7) to remove the free hydrocarbons. Analyses of $\delta^{13}\text{C}$ ratios were performed using a GV Instruments Isoprime EA mass spectrometer (precision of the $\delta^{13}\text{C}$ measurements: $\pm 0.10\%$). The $\delta^{13}\text{C}$ ratios were expressed as permil deviation from the Pee Dee Belemnite (PDB) standard.

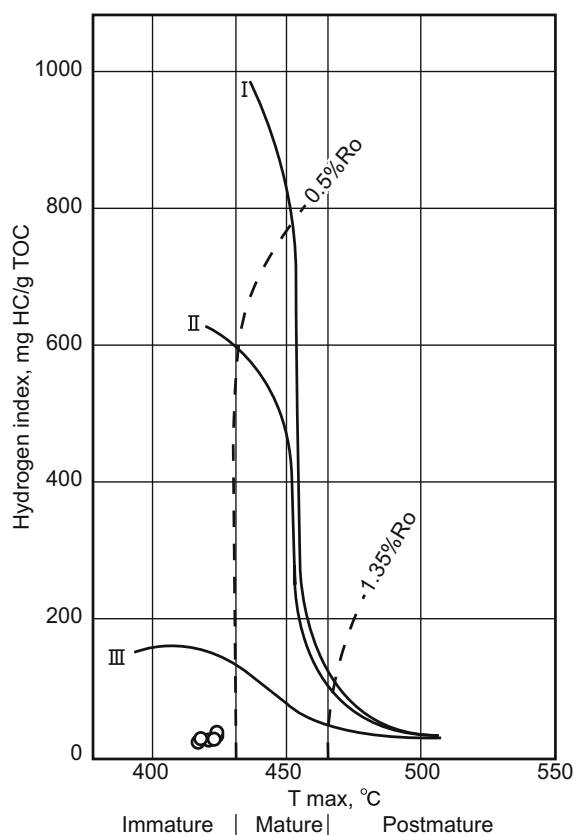
RESULTS

Kerogen type and thermal maturity of organic matter

The results of the TOC content analysis and the Rock-Eval pyrolysis are shown in Table 1, and plots of the Hydrogen Index versus the T_{max} are shown in Text-fig. 3. These ranges are applicable to the type III kerogen, and the T_{max} values indicate immaturity.

Sample	TOC (%)	S1 (mg/g)	S2 (mg/g)	S3 (mg/g)	HI (mg HC/g TOC)	OI (mg HC/g TOC)	T_{max} (°C)
OFM 4	0.63	0.02	0.21	0.14	33	22	424
OFM 33	0.81	0.09	0.31	0.29	38	36	424
CMI 50	0.75	0.02	0.18	0.36	24	48	417
CMI 44	0.66	0.02	0.18	0.36	27	55	421
CMI 26	0.88	0.02	0.25	0.37	28	42	423
CMI 22	0.66	0.02	0.19	0.37	29	56	418

Table 1. Total organic carbon contents and Rock-Eval pyrolysis of the selected samples. The three letter initials are the same as those in Text-fig. 2



Text-fig. 3. Plot of the Hydrogen Index versus the T_{max} of selected mudstone samples in the Haboro and Obira area. Ro: Vitrinite Reflectance

Carbon isotope values

The $\delta^{13}C_{org}$ values of organic matter ($\delta^{13}C_{org}$) range from -24.9‰ to -23.3‰ in the Haboro area and from -24.9‰ to -23.9‰ in the Obira area (Table 2, Text-figs. 4, 5).

In the Haboro area, the $\delta^{13}C_{org}$ profile shows a positive shift, including fluctuations of $\sim 0.5\text{‰}$, up to an horizon between the sandstone key beds of MHs5 and UHs1. The $\delta^{13}C_{org}$ values vary from -24.9‰ to -22.9‰. Thereafter, the $\delta^{13}C_{org}$ profile shows a negative shift, including some fluctuations of $\sim 0.5\text{‰}$, in the uppermost part of the Haborogawa Formation.

In the Obira area, a positive anomaly of 0.6‰ characterises the lowermost part of the Haborogawa Formation. The $\delta^{13}C_{org}$ profile shows a negative shift of 0.9‰ in the uppermost part of the Kamikinenbetsu Sandstone Member. The $\delta^{13}C_{org}$ profile then shows a positive shift of 0.9‰, including two positive peaks, in the lower part of the Haborogawa Formation.

Inoceramid biostratigraphy

The Haboro area along the Haboro River and its tributaries; The Saku Formation

The inoceramid reported in the Saku Formation is *Inoceramus teshioensis* Nagao and Matsumoto, the lowest occurrence of which is in the upper part of this formation (Okamoto *et al.* 2003; Text-fig. 4).

The Haboro area along the Haboro River and its tributaries; The Haborogawa Formation

The highest occurrence of *I. teshioensis* is ~ 150 m above the basal part of the Haborogawa Formation (Okamoto *et al.*, 2003). The lowest occurrence of *I. uwajimensis* Yehara was reported by Okamoto *et al.* (2003) to be ~ 150 m above the basal part of this formation along the Takemizawa River branch of the Sakasa River. *I. pedalionoides* Nagao and Matsumoto and *I. uwajimensis* were collected from the lower part of the formation along the Chimeizawa River and *Platyceramus szaszi* (Noda and Uchida) from the lower part of the formation along the Haboro River. The lowest occurrence of *Cremnoceramus mihoensis* (Matsumoto) was reported by Okamoto *et al.* (2003) to be ~ 300 m above the basal part of this formation along the Nakanofutamata River. The lowest occurrence of *Cordiceramus kawashitai* (Noda) is ~ 450 m above the basal part of this formation along the Chimeizawa River. The lowest occurrence of *Sphenoceramus naumanni* (Yokoyama) was reported by Toshimitsu (1988) near the horizon of the highest occurrence of *Cr. mihoensis* ~ 600 m above the basal part of this formation, and the species ranges up to the highest part of the formation. Although *Inoceramus amakusensis* Nagao and Matsumoto was not obtained in this study, the lowest occurrence of this species was reported by Okamoto *et al.* (2003) to be ~ 650 m above the basal part of this formation and the highest occurrence mentioned by Toshimitsu (1988) was just below the sandstone key bed UHs1. The lowest occurrence of *Platyceramus mantelli* (De Mercey) was reported by Toshimitsu (1988) at 340 m below the sandstone key bed MHs4 and the highest occurrence was confirmed near the UHs1 key bed in this study. The lowest occurrence of *Platyceramus ezoensis* (Yokoyama) is at ~ 50 m above UHs1 (Toshimitsu 1988), and the highest occurrence is in the highest part of this formation. The lowest occurrence of *Platyceramus japonicus* (Nagao and Matsumoto) was reported by Moriya and Hirano (2001) just above the UHs1. Toshimitsu (1988) reported the occurrence of *Sphenoceramus schmidtii* (Michael) in the topmost part of the Haborogawa Formation (Text-fig. 4).

Sample	$\delta^{13}\text{C}$ (‰)	Sample	$\delta^{13}\text{C}$ (‰)	Sample	$\delta^{13}\text{C}$ (‰)	Sample	$\delta^{13}\text{C}$ (‰)	Sample	$\delta^{13}\text{C}$ (‰)
CMI 10	-23.92	CMI 20	-23.63	CMI 30	-22.89	CMI 40	-23.68	CMI 51	-24.19
CMI 9	-23.96	CMI 19	-23.76	CMI 29	-23.76	CMI 39	-23.88	CMI 50	-23.96
CMI 8	-23.71	CMI 18	-23.48	CMI 28	-23.33	CMI 38	-24.04	CMI 49	-23.94
CMI 7	-24.02	CMI 17	-23.73	CMI 27	-23.87	CMI 37	-23.78	CMI 48	-23.83
CMI 6	-24.44	CMI 16	-24.08	CMI 26	-23.20	CMI 36	-23.55	CMI 47	-24.19
CMI 5	-24.20	CMI 15	-24.21	CMI 25	-23.26	CMI 35	-23.61	CMI 46	-24.17
CMI 4	-24.02	CMI 14	-23.88	CMI 24	-23.22	CMI 34	-23.29	CMI 45	-23.83
CMI 3	-23.91	CMI 13	-23.80	CMI 23	-23.31	CMI 33	-23.09	CMI 44	-23.80
CMI 2	-24.37	CMI 12	-23.92	CMI 22	-23.95	CMI 32	-23.34	CMI 43	-23.35
CMI 1	-24.91	CMI 11	-24.16	CMI 21	-23.88	CMI 31	-23.30	CMI 42	-23.76
								CMI 41	-23.37
OFM 10	-24.80	OFM 20	-24.06	OFM 30	-24.04	OFM 34	-24.14		
OFM 9	-24.90	OFM 19	-24.18	OFM 29	-24.06	OFM 33	-24.25		
OFM 8	-24.79	OFM 18	-24.43	OFM 28	-24.07	OFM 32	-24.18		
OFM 7	-24.72	OFM 17	-24.37	OFM 27	-24.32	OFM 31	-23.98		
OFM 6	-24.62	OFM 16	-24.52	OFM 26	-24.35				
OFM 5	-24.85	OFM 15	-24.32	OFM 25	-24.20				
OFM 4	-24.21	OFM 14	-24.40	OFM 24	-24.65				
OFM 3	-24.75	OFM 13	-24.61	OFM 23	-23.97				
OFM 2	-24.09	OFM 12	-24.58	OFM 22	-24.36				
OFM 1	-24.73	OFM 11	-24.53	OFM 21	-24.27				
OBR 10	-24.12	OBR 20	-24.60	OBR 30	-24.61	OBR 41	-24.68		
OBR 9	-24.33	OBR 19	-24.33	OBR 29	-24.40	OBR 40	-24.69		
OBR 8	-24.22	OBR 18	-24.31	OBR 28	-24.42	OBR 39	-24.78		
OBR 7	-24.02	OBR 17	-24.52	OBR 27	-24.60	OBR 38	-24.60		
OBR 6	-24.24	OBR 16	-24.13	OBR 26	-24.50	OBR 37	-24.64		
OBR 5	-24.53	OBR 15	-23.96	OBR 25	-24.27	OBR 36	-24.52		
OBR 4	-24.31	OBR 14	-24.21	OBR 24	-24.25	OBR 35	-24.78		
OBR 3	-24.53	OBR 13	-24.17	OBR 23	-24.27	OBR 34	-24.79		
OBR 2	-24.29	OBR 12	-24.19	OBR 22	-24.22	OBR 33	-23.89		
OBR 1	-24.46	OBR 11	-24.11	OBR 21	-24.21	OBR 32	-24.69		
						OBR 31	-24.37		

Table 2. Carbon isotope values in the study sections. The three letter initials are the same as those in Text-fig. 2

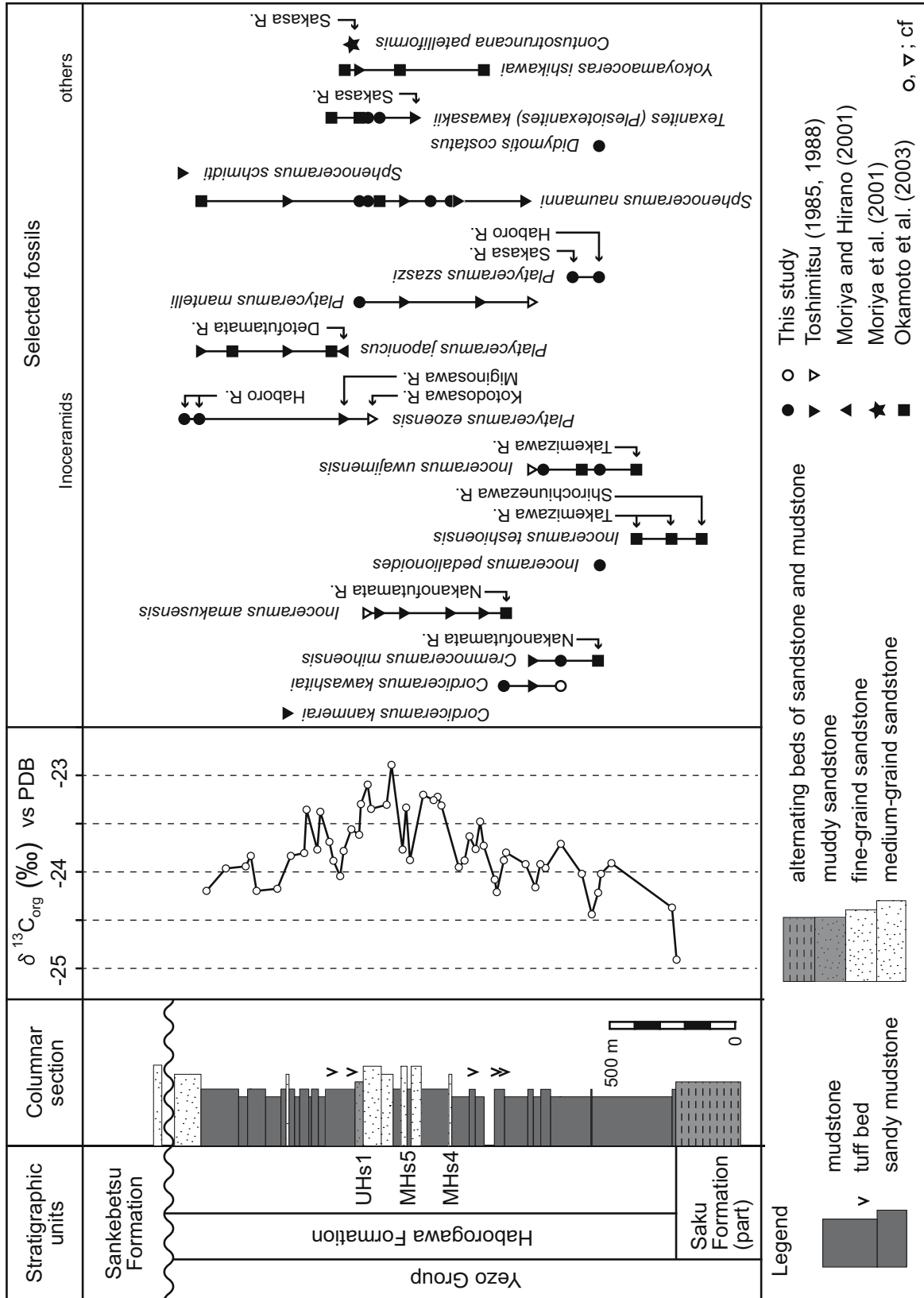
The Obira area along the Obirashibe River and its tributaries; The Saku Formation

Tanabe *et al.* (1977) reported the lowest occurrence of *Inoceramus teshioensis* and *Inoceramus pedalionoides* Nagao and Matsumoto, and Sekine *et al.* (1985) reported the lowest occurrence of *Inoceramus tenuistriatus* Nagao and Matsumoto (Text-fig. 5, 6) in the upper part of the Saku Formation.

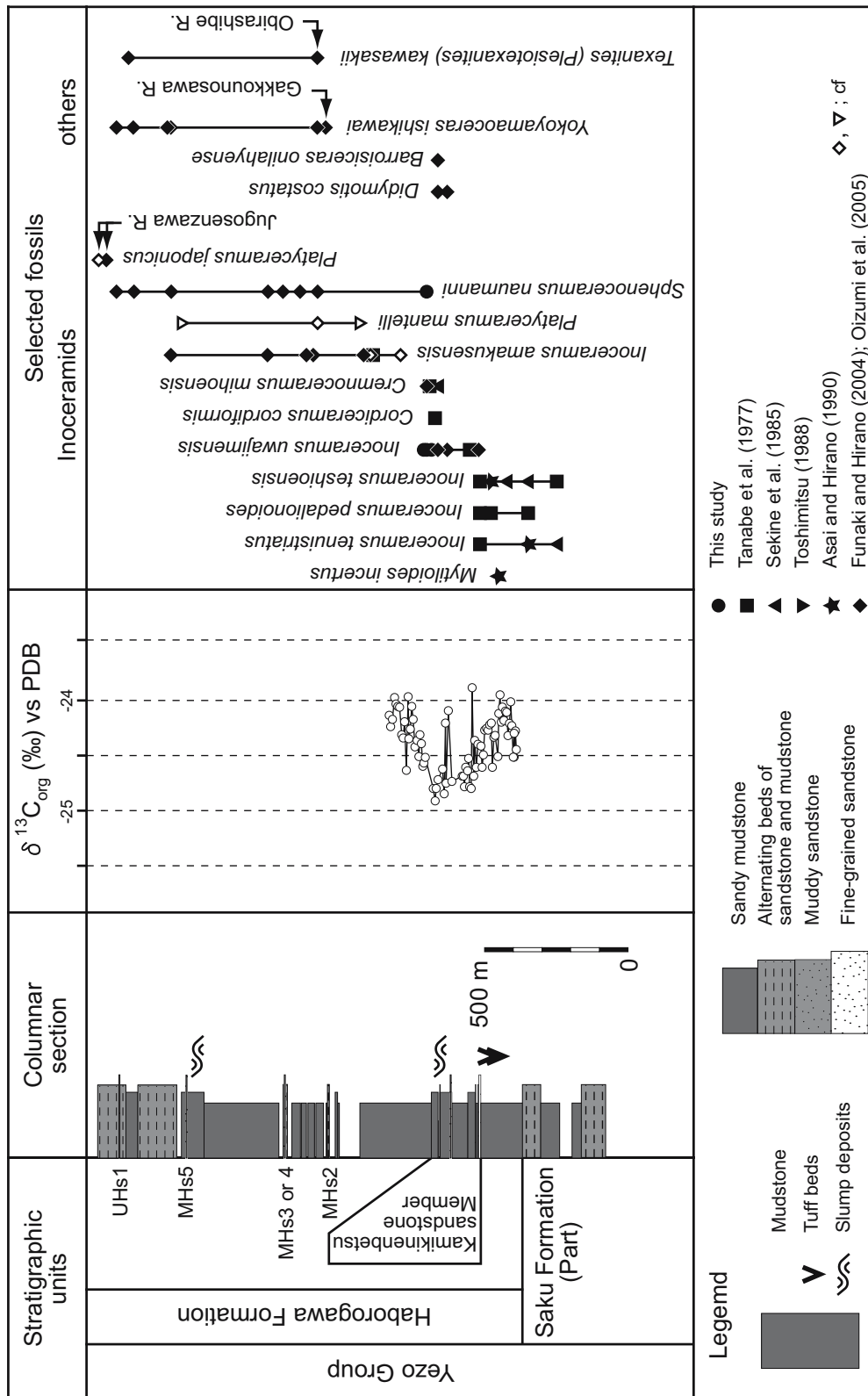
The Obira area along the Obirashibe River and its tributaries; The Haborogawa Formation

I. pedalionoides, *I. tenuistriatus* and *I. teshioensis* occur successively in the lowermost part of the Haborogawa Formation (Tanabe *et al.* 1977; Sekine *et al.* 1985; Asai and Hirano 1990). Asai and Hirano (1990) reported the occurrence of the Upper Turonian species

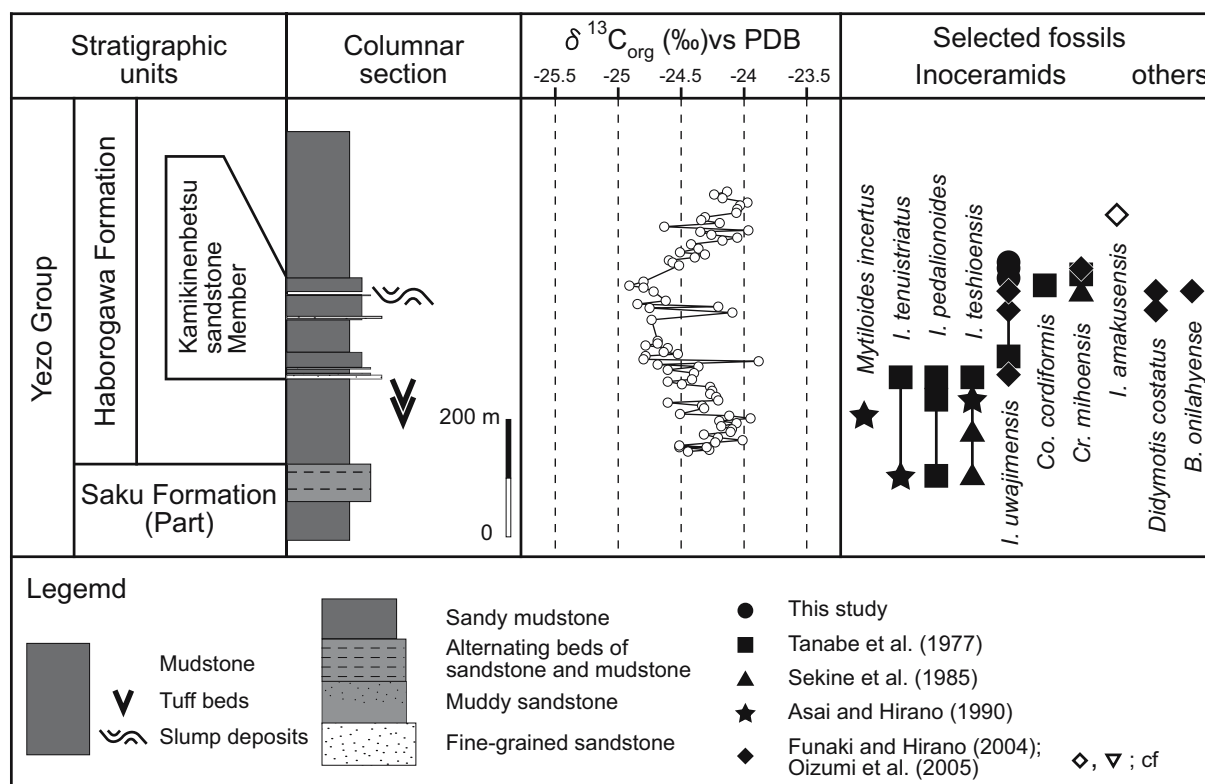
Mytiloides incertus (Jimbo) in the lowermost part of the formation. The lowest occurrence of *I. uwajimensis* is just below the Kamikinenbetsu Sandstone Member (Funaki and Hirano, 2004). The lowest occurrence of both *Cr. mihoensis* (Sekine *et al.* 1985) and *Cordiceramus cordiformis* (J. de C. Sowerby) (Tanabe *et al.* 1977) are in the uppermost part of the Kamikinenbetsu Sandstone Member. These two species occur successively up to just above the Kamikinenbetsu Sandstone Member. The highest occurrence of *Cr. mihoensis* is near the lowest occurrence of *S. naumanni*, which ranges up to the highest part of this formation. The lowest occurrence of *I. amakusensis* is ~500 m above the basal part of this formation (Oizumi *et al.* 2005), and the highest occurrence is just below the UHs1 key bed. The lowest occurrence of *P. cf. mantelli* is 100 m below the MHs2 key bed, and the highest occurrence is near the MHs5 key bed (Toshimitsu 1988).



Text-fig. 4. Columnar section of the $\delta^{13}C_{org}$ profile and the distribution of selected fossils in the Haboro area. Names of the rivers are mentioned in their occurrence out of this section. MHs4-5 and UHs1 are the key-marker-beds of Toshimitsu (1988)



Text-fig. 5. Columnar section of the $\delta^{13}C_{org}$ profile and the distribution of selected fossils in the Obira area. The columnar section is modified after Funaki and Hirano (2004) and Oizumi *et al.* (2005). Names of the rivers are mentioned in their occurrence out of this section. MHs4-5 and UHs1 are the key-marker-beds of Toshimitsu (1988)



Text-fig. 6. Enlarged columnar section of the $\delta^{13}\text{C}_{\text{org}}$ profile and the distribution of selected fossils in the Obira area. The columnar section is modified after Funaki and Hirano (2004) and Oizumi *et al.* (2005)

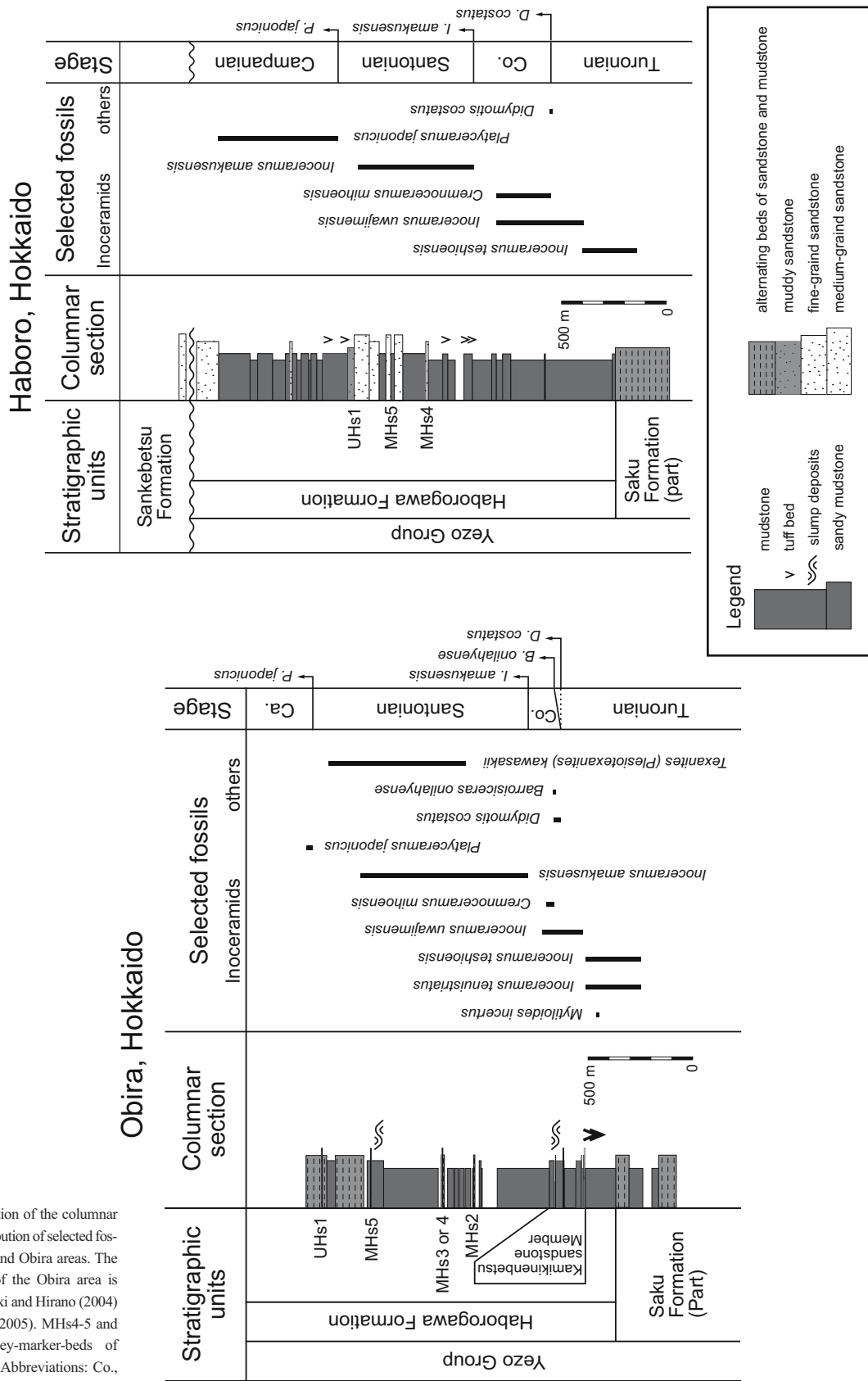
Stratigraphic distributions and geological ages in previous studies

The Saku and Haborogawa Formations yield well-preserved, abundant macro- and microfossils documented in many biostratigraphic studies (Tanaka 1963; Tanabe *et al.* 1977; Sekine *et al.* 1985; Toshimitsu 1985, 1988, Toshimitsu *et al.* 1998; Okamoto *et al.* 2003; Funaki and Hirano 2004; Oizumi *et al.* 2005). According to these studies, the sections have been correlated with macrofossils and range from the upper Turonian to the lower Campanian. The Turonian/Coniacian boundary is located in the lowest part of the Haborogawa Formation and has been defined by the lowest occurrence of the inoceramids *Didymotis costatus* and the occurrence of the ammonoid *Barroisiceras onilahyense* (Funaki and Hirano 2004) (Text-fig.7). The Coniacian/Santonian boundary is located in the lower part of the Haborogawa Formation and has been defined by the lowest occurrence of *I. amakusensis* (Toshimitsu 1988; Toshimitsu *et al.* 1995; Oizumi *et al.* 2005) (Text-fig.7). The Santonian/Campanian boundary is located in the upper part of the Haborogawa Formation and has been defined by the lowest occurrence of *Platyceramus japonicus* (Toshimitsu *et al.* 1995; Oizumi *et al.* 2005) (Text-fig.7).

Inoceramid biozones

Funaki and Hirano (2004) recognised 7 inoceramid biozones in the Obira area by using inoceramid species that Toshimitsu *et al.* (1995) defined as inoceramid zonal indices. These biozones are as follows, in ascending order: 1) the *Inoceramus virgatus* Interval Zone; 2) the *Actinoceramus* sp. ex. gr. *nipponicus* Interval Zone; 3) the *Inoceramus kamuy* Interval Zone; 4) the *Inoceramus hobetsensis* Interval Zone; 5) the *Inoceramus hobetsensis*-*Inoceramus teshioensis* Concurrent-range Zone; 6) the *Inoceramus teshioensis* Partial-range Zone; and 7) the *Inoceramus uwajimensis* Interval Zone.

In this study, we recognise 4 inoceramid biozones above the *I. teshioensis* Partial-range Zone in both areas by using inoceramid species that Toshimitsu *et al.* (1995) defined as inoceramid zonal indices. These biozones are as follows, in ascending order: 1) the *Inoceramus uwajimensis* Interval Zone (redefined), which is defined in this study as the stratigraphic interval from the lowest occurrence of *I. uwajimensis* to the lowest occurrence of *Cremnoceramus mihoensis*; 2) the *Cremnoceramus mihoensis* Interval Zone, which is defined as the stratigraphic interval from the lowest occurrence of *Cr. mihoensis* to the lowest occurrence of *Inocera-*



Text-fig. 7. Correlation of the columnar sections of the distribution of selected fossils in the Haboro and Obira areas. The columnar section of the Obira area is modified after Funaki and Hirano (2004) and Oizumi *et al.* (2005). MHs4-5 and UHs1 are the key-marker-beds of Toshimitsu (1988). Abbreviations: Co., Coniacian; Ca., Campanian

mus amakusensis; 3) the *Inoceramus amakusensis* Interval Zone, which is defined as the stratigraphic interval from the lowest occurrence of *I. amakusensis* to the lowest occurrence of *Platyceramus japonicus*; and 4) the *Platyceramus japonicus* Interval Zone, which is defined as the stratigraphic interval from the lowest occurrence of *P. japonicus* to the lowest occurrence of *Sphenoceramus schmidtii*.

DISCUSSION

Evaluation of sedimentary organic matter

The sedimentary organic matter in the mudstone samples is a type III kerogen (Text-fig. 3), which means that the organic matter originated from terrestrial plants (Hunt 1996). The $\delta^{13}\text{C}$ values of kerogen change are known in the metamorphic stage but not below that stage (Whiticar 1996). The kerogen in the mudstone samples has not experienced the metamorphic stage according to the T_{max} values (Hunt 1996), thus the $\delta^{13}\text{C}$ records are not influenced by thermal maturity. Therefore, the $\delta^{13}\text{C}$ values of the kerogen in our samples represent the values of the original terrestrial organic matter (TOM). We recognize that the changes of the vegetation in the hinterland may have some influence. Therefore we pay attention to the general trend and amplitude of the measured values.

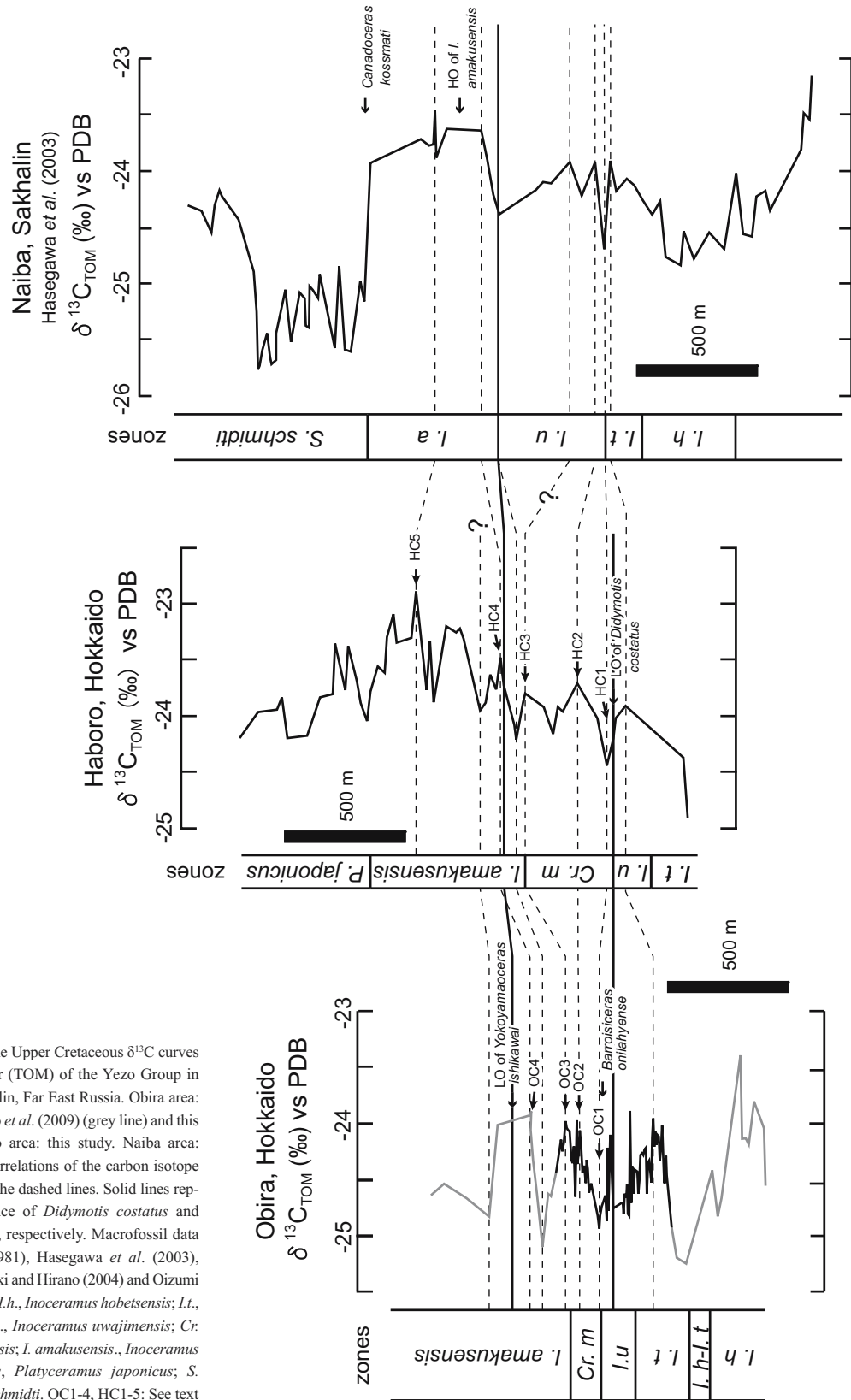
Correlation of $\delta^{13}\text{C}_{\text{TOM}}$ profiles in the Yezo Group

Uramoto *et al.* (2009) showed the intrabasinal correlation of the $\delta^{13}\text{C}_{\text{TOM}}$ profile obtained in the Obira area with those of the previous studies (Kotanbetsu section: Hasegawa and Hatsugai 2000; Oyubari section: Hasegawa 1997, Tsuchiya *et al.* 2003; Naiba section (Sakhalin): Hasegawa *et al.* 2003) based on the occurrence of the global age-diagnostic macro- and microfossils and biohorizons of the regional marker inoceramids. Uramoto *et al.* (2009) demonstrated that the $\delta^{13}\text{C}_{\text{TOM}}$ profiles show notable fluctuations at specific stratigraphic horizons and that the $\delta^{13}\text{C}_{\text{TOM}}$ values and the amplitudes of the fluctuations in different Yezo Group sections are similar.

We correlated the $\delta^{13}\text{C}_{\text{TOM}}$ profiles between the Haboro area, the Obira area, and the Naiba area of Sakhalin from Hasegawa *et al.* (2003) (Text-fig. 8). The $\delta^{13}\text{C}_{\text{TOM}}$ profiles for the Obira area in this study and that of Uramoto *et al.* (2009) were integrated because the $\delta^{13}\text{C}_{\text{TOM}}$ profile in this study overlaps with part of the profile of Uramoto *et al.* (2009) and the fluctuation patterns of these profiles are the same in the over-

lapped section along the Obirashibe and Okufutamatanzawa rivers. The lowest occurrences of the ammonoid *Yokoyamaoceras ishikawai* (Jimbo) and the inoceramid bivalve *Didymotis costatus* (Fric) were used as regional stratigraphic markers to correlate the $\delta^{13}\text{C}_{\text{TOM}}$ profiles of these three areas. The lowest occurrence of *D. costatus* can be used for correlation as a stratigraphic marker near the Turonian/Coniacian boundary in the Obira area (Funaki and Hirano 2004). We collected *D. costatus* in the Chimeizawa River in the Haboro area (Text-fig. 4), and we were able to recognise the same horizon in both the Haboro and Obira areas. The lowest occurrence of *Y. ishikawai* can be used for correlation as a biostratigraphic marker because the species occurs continuously from the Santonian to the Campanian in the Yezo Group (e.g., Oizumi *et al.* 2005).

The $\delta^{13}\text{C}_{\text{TOM}}$ profiles show a negative excursion of 0.5‰ (HC1) in the Haboro area and of 0.9‰ (OC1) in the Obira area near the lowest occurrence of *D. costatus*, and a positive excursion of 1.0‰ (HC2) in the Haboro area and of 0.9‰ (OC2) in the Obira area above the horizon of the previously-mentioned negative excursion (Text-fig. 8). These $\delta^{13}\text{C}_{\text{TOM}}$ fluctuations were also recognised in the Naiba area of Sakhalin by Hasegawa *et al.* (2003), albeit *D. costatus* was not found (Text-fig. 8). The correlation of these positive-negative $\delta^{13}\text{C}_{\text{TOM}}$ fluctuations was carried out by Uramoto *et al.* (2009), and it was confirmed that these fluctuations can be correlated between the Haboro, Obira and Naiba areas. The small positive peaks (HC3, OC3) were correlated between the Haboro and Obira areas because the amplitudes of these peaks are the same in both areas. The positive shift (HC4, OC4) is near the lowest occurrence of *Yokoyamaoceras ishikawai* in all three areas (Text-fig. 8). The amplitude of this shift is 0.7‰ (HC4) in the Haboro area, 1.2‰ (OC4) in the Obira area and 0.8‰ in the Naiba area (Hasegawa *et al.* 2003), respectively. It is considered that this positive shift and the negative shifts accompanied by a positive shift are correlatable fluctuations between the three areas. Our correlation of these fluctuations agrees with that of Uramoto *et al.* (2009). A long-term trend of the $\delta^{13}\text{C}_{\text{TOM}}$ curve of the Haboro area shows a positive shift including small fluctuation above the lowest occurrence of *Y. ishikawai*. A maximum value of -22.9‰ (HC5) is recognised in the upper part of the *I. amakusensis* Interval Zone of the Haboro area, and the trend becomes negative above this horizon. These trends are comparable with the $\delta^{13}\text{C}_{\text{TOM}}$ profile of the Naiba area in Sakhalin from Hasegawa *et al.* (2003) (Text-fig. 8). However, this suggested isotopic correlation cannot be confirmed because there is inadequate biostratigraphic correlation be-



Text-fig. 8. Correlation of the Upper Cretaceous $\delta^{13}\text{C}$ curves of terrestrial organic matter (TOM) of the Yezo Group in Hokkaido, Japan and Sakhalin, Far East Russia. Obira area: composite curve of Uramoto *et al.* (2009) (grey line) and this study (black line); Haboro area: this study. Naiba area: Hasegawa *et al.* (2003). Correlations of the carbon isotope fluctuations are marked by the dashed lines. Solid lines represent the lowest occurrence of *Didymotis costatus* and *Yokoyamaoceras ishikawai*, respectively. Macrofossil data after Matsumoto *et al.* (1981), Hasegawa *et al.* (2003), Okamoto *et al.* (2003), Funaki and Hirano (2004) and Oizumi *et al.* (2005). Abbreviations: *l.h.*, *Inoceramus hobetsensis*; *l.t.*, *Inoceramus teshioensis*; *l.u.*, *Inoceramus uwajimensis*; *Cr. m.*, *Cremnoceramus mihoensis*; *l. amakusensis.*, *Inoceramus amakusensis*; *P. japonicus*, *Platyceramus japonicus*; *S. schmidtii*, *Sphenoceramus schmidtii*. OC1-4, HC1-5: See text

tween the two areas, the relevant stratigraphic marker fossils having not so far been found in the Naiba section. The two $\delta^{13}\text{C}_{\text{TOM}}$ profiles in this study are identical in the patterns of fluctuation and amplitude to each other and are similar to the profile of the Naiba area in Sakhalin from Hasegawa *et al.* (2003). Thus, the $\delta^{13}\text{C}_{\text{TOM}}$ fluctuations in this study were interpreted to represent the averaged $\delta^{13}\text{C}_{\text{TOM}}$ fluctuations of the Yezo Group.

Relationship between the carbon isotope fluctuations and the occurrence of inoceramids

It is demonstrated that the $\delta^{13}\text{C}_{\text{TOM}}$ profiles can be correlated between Yezo Group sections and that positive and negative spikes and shifts in isotopic values can be used as chemostratigraphic datum levels in the Haboro and Obira areas. The relationship between the $\delta^{13}\text{C}_{\text{TOM}}$ profiles and the occurrence of inoceramids is shown in Text-fig. 9.

The lowest occurrence of the inoceramid *Didymotis costatus* is in the basal part of the *Cr. mihoensis* Interval Zone in the Haboro area and in the middle part of the *I. uwajimensis* Interval Zone in the Obira area. The negative peaks of the $\delta^{13}\text{C}_{\text{TOM}}$ profiles (HC1 and OC1) are in the lowest part of the *Cr. mihoensis* Interval Zone in both areas (Text-fig 9). The lowest occurrence of the ammonoid *Yokoyamaoceras ishikawai* is in the lower part of the *I. amakusensis* Interval Zone in both areas. The HC3 positive peak is in the basal part of the *I. amakusensis* Interval Zone in the Haboro area and the corresponding OC3 peak is in the lowest part of *I. amakusensis* Interval Zone in the Obira area. The timing of the occurrence of inoceramids in the range from the *I. uwajimensis* Interval Zone to the *I. amakusensis* Interval Zone in the Haboro and Obira areas corresponds well, and the occurrence of *Inoceramus pedalionoides* and *Platyceramus mantelli*, which occur less commonly in these areas, is only different between these two areas based on the correlation of the $\delta^{13}\text{C}_{\text{TOM}}$ fluctuations. *I. pedalionoides* ranges from the *I. teshioensis* Partial-range Zone to the *I. uwajimensis* Interval Zone, and *P. mantelli* from the *Cr. mihoensis* Interval Zone to the *I. amakusensis* Interval Zone (Noda and Matsumoto 1998; Toshimitsu *et al.* 2007). However, the difference in occurrence of these two rare species would not be inconsistent with the correlation of the $\delta^{13}\text{C}_{\text{TOM}}$ profiles. Therefore, it is demonstrated that the $\delta^{13}\text{C}_{\text{TOM}}$ profiles of the Haboro and Obira areas, which are correlated by *Didymotis costatus* and *Yokoyamaoceras ishikawai*, are consistently correlated by inoceramids except for the rare occurrence of *I. pedalionoides* and *P. mantelli*.

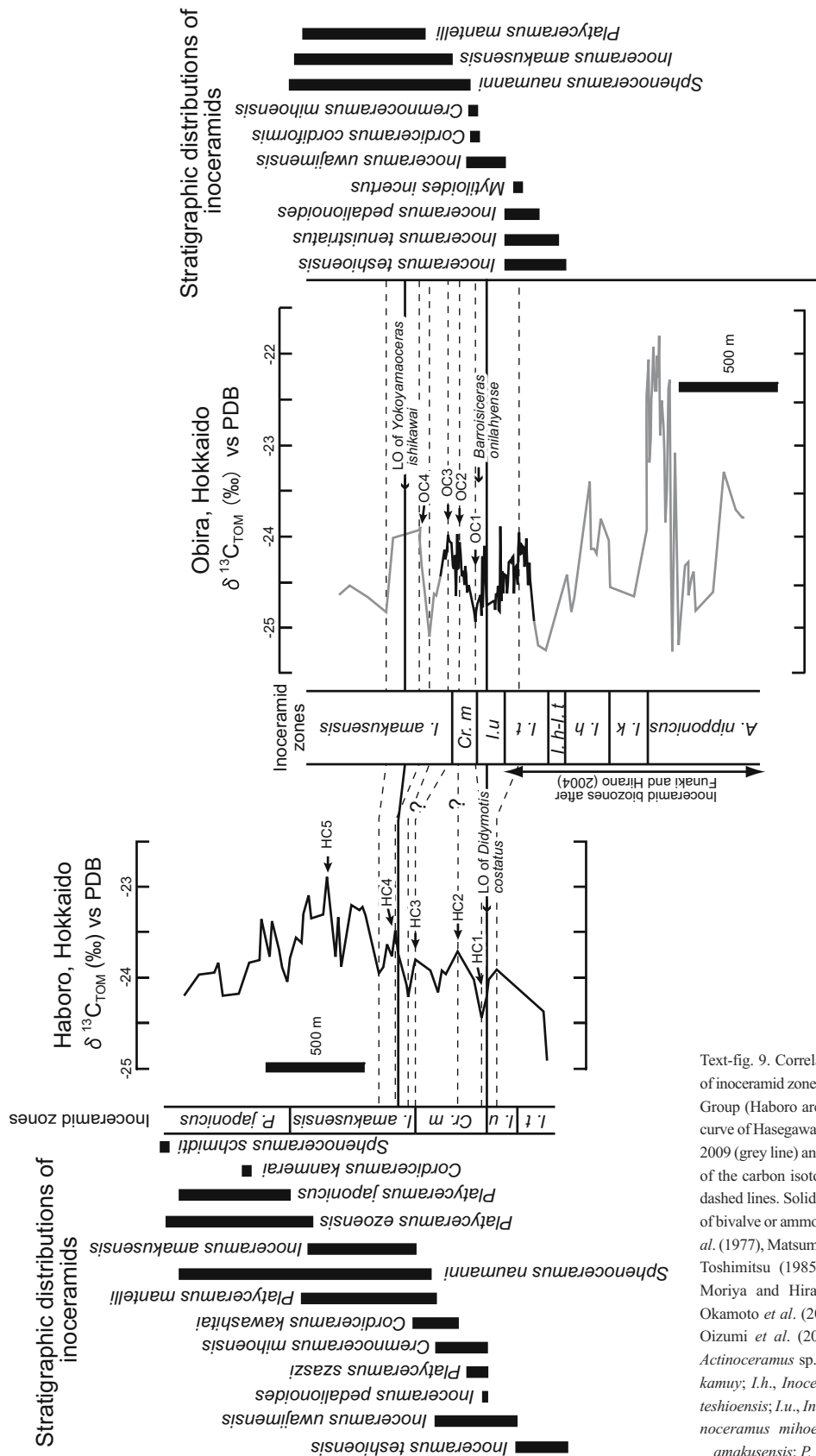
$\delta^{13}\text{C}$ correlation between terrestrial organic matter of the Yezo Group and marine carbonate of the European sections

The $\delta^{13}\text{C}_{\text{TOM}}$ profiles and the inoceramid biozones in the Haboro and the Obira areas were integrated to correlate the terrestrial organic $\delta^{13}\text{C}$ fluctuation with the marine carbonate $\delta^{13}\text{C}$ record in Europe. The recognisable positive and negative isotope peaks are designated H1 to H13, in ascending stratigraphic order (Text-fig. 10, 11).

The $\delta^{13}\text{C}_{\text{TOM}}$ profile in the *I. teshioensis* Partial-range Zone is characterised by a negative peak (H1) from Uramoto *et al.* (2009) in the lowest part and a positive peak (H2) in the upper part (Text-fig. 10, 11). These two peaks lie between the occurrences of *Subprionocyclus cf. neptuni* and *D. costatus* that are correlated with the Upper Turonian. Therefore, the H1 and H2 peaks are correlated with the Bridgewick Isotope Event (Jarvis *et al.* 2006) and the Hitch Wood Isotope Event (Gale 1996) respectively (Text-fig. 10, 11).

The $\delta^{13}\text{C}_{\text{TOM}}$ profile shows a negative shift above the H2 positive peak from the upper part of the *I. teshioensis* Partial-range Zone to the *I. uwajimensis* Interval Zone. The occurrence of *D. costatus* is in this interval.

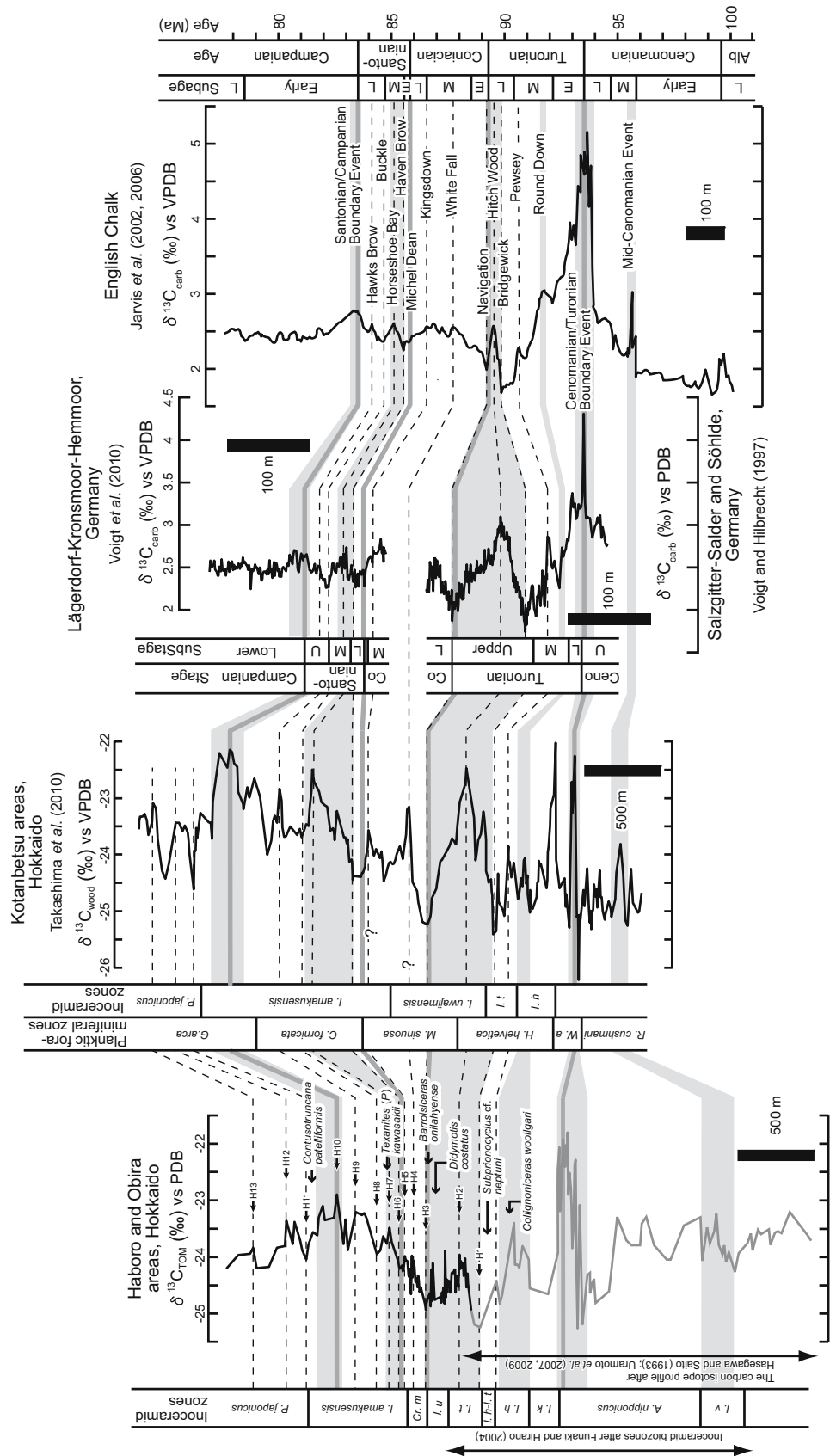
The Upper Turonian strata are characterised by two *Didymotis* Events (Wood *et al.* 1984, 2004; Kauffman *et al.* 1996) in Europe. The *Didymotis* Events in Europe lie between the Hitch Wood and Navigation isotope events (Jarvis *et al.* 2006). In the *Cr. mihoensis* Interval Zone, the $\delta^{13}\text{C}_{\text{TOM}}$ curve consists of a negative peak (H3) in the basal part and a positive peak (H4) in the upper part (Text-fig. 10, 11). In the Obira area, the lowest occurrence of *D. costatus* lies between the Hitch Wood Event and the H3 negative peak. Therefore, the H3 negative peak, which lies above the correlative of the Hitch Wood Event in the basal part of the *Cr. mihoensis* Interval Zone, is correlated with the Navigation Isotope Event in the English Chalk (Jarvis *et al.* 2006) (Text-figs 10, 11). The Navigation Event characterises the Turonian/Coniacian boundary (Jarvis *et al.* 2006), and the *I. uwajimensis* Interval Zone is correlated with the upper Upper Turonian. The H4 positive peak in the upper part of the *Cr. mihoensis* Interval Zone probably correlates with the White Fall Isotope Event (Jarvis *et al.* 2006) in the lower Middle Coniacian, albeit this correlation is not supported by the biostratigraphic calibration. We correlate the *Cr. mihoensis* Interval Zone with the Lower Coniacian to the Middle Coniacian, albeit the stratigraphic interval with the occurrence of *Cr. mihoensis* was hitherto correlated with the upper Coniacian (Toshimitsu *et al.* 1995).



Text-fig. 9. Correlation of the stratigraphic distribution of inoceramid zones and the $\delta^{13}\text{C}_{\text{TOM}}$ curves of the Yezo Group (Haboro area: this study; Obira area: composite curve of Hasegawa and Saito, 1993; Uramoto *et al.* 2007, 2009 (grey line) and this study (black line)). Correlations of the carbon isotope fluctuations are indicated by the dashed lines. Solid lines represent the lowest occurrence of bivalve or ammonoid. Macrofossil data after Tanabe *et al.* (1977), Matsumoto *et al.* (1981), Sekine *et al.* (1985), Toshimitsu (1985, 1988), Asai and Hirano (1990), Moriya and Hirano (2001), Moriya *et al.* (2001), Okamoto *et al.* (2003), Funaki and Hirano (2004) and Oizumi *et al.* (2005). Abbreviations: *A. nipponicus*, *Actinoceras* sp. ex gr. *nipponicus*; *I. k.*, *Inoceramus kamuyi*; *I. h.*, *Inoceramus hobetsensis*; *I. t.*, *Inoceramus teshioensis*; *I. u.*, *Inoceramus uwajimensis*; *Cr. m.*, *Cremnoceras mihoensis*; *I. amakusensis.*, *Inoceramus amakusensis*; *P. japonicus*, *Platyceras japonicus*

REVISED INOCERAMID BIOZONATION FOR THE UPPER CRETACEOUS OF JAPAN

Text-fig. 10. Correlation of the carbon isotope stratigraphy between the Haboro and Obira areas (this study; Hasegawa and Saito 1993; Uramoto *et al.* 2007, 2009), Kotanbetsu area (Takashima *et al.* 2010), Salzgitter Salder and Söhlde section (Voigt and Hilbrecht 1997), Lägerdorf-Kronsmoor-Hemmoor succession (Voigt *et al.* 2010) and the English Chalk (Jarvis *et al.* 2002, 2006). Correlations of the carbon isotope fluctuations are indicated by the grey bands and dashed lines. Macrofossil data after Tanabe *et al.* (1977), Matsumoto *et al.* (1981), Toshimitsu (1985, 1988) and Moriya *et al.* (2001). The lower limit of the *I. amakusensis* zone of Takashima *et al.* (2010) is revised after Hirano *et al.* (2011). Abbreviations: *I. v.*, *Inoceramus virgatus*; *A. nipponicus*, *Actinoceramus* sp. ex gr. *nipponicus*; *I. k.*, *Inoceramus kamuyi*; *I. h.*, *Inoceramus hobetsensis*; *I. t.*, *Inoceramus teshioensis*; *I. u.*, *Inoceramus uwajimensis*; *Cr. m.*, *Cremnoceramus mihoensis*; *I. amakusensis*, *Inoceramus amakusensis*; *P. japonicus*, *Platyceramus japonicus*; *R. cushmani*, *Rotalipora cushmani*; *W. a.*, *Whiteinella archaeoetacea*; *H. helvetica*, *Helvetoglobotruncana helvetica*; *M. sinuosa*, *Marginotruncana sinuosa*; *C. fornicata*, *Contusotruncana fornicata*; *G. arca*, *Globotruncana arca*; Alb., Albian; Ceno., Cenomanian; Co., Coniacian



The $\delta^{13}\text{C}_{\text{TOM}}$ curve in the lower part of the *I. amakusensis* Interval Zone is characterised by two positive peaks (H5 and H7) and a negative peak (H6). The $\delta^{13}\text{C}_{\text{carb}}$ curve rises above the Navigation Event, with short-term fluctuations, and reaches a maximum at the Middle/Upper Coniacian boundary. This $\delta^{13}\text{C}$ maximum is the Kingsdown Isotope Event (Jarvis *et al.* 2006). The $\delta^{13}\text{C}_{\text{carb}}$ values then fall throughout the Upper Coniacian to Lower Santonian both in England (Jarvis *et al.* 2006) and in Germany (Voigt *et al.* 2010). The $\delta^{13}\text{C}_{\text{TOM}}$ values, conversely, rise in the *Cr. mihoensis* Interval Zone, reaching a maximum (H5) in the basal part of the *I. amakusensis* Interval Zone and display a negative shift above the H5 positive peak. This trend of the $\delta^{13}\text{C}_{\text{TOM}}$ curves is similar to the $\delta^{13}\text{C}_{\text{carb}}$ curve, thus the H5 positive peak, in the lowest part of the *I. amakusensis* Interval Zone, correlates with the Kingsdown Isotope Event (Text-fig. 10, 11). A small positive peak between H5 and H6 probably correlates with the Michel Dean Isotope Event, which is very close to the base of the Santonian (Jarvis *et al.* 2006) (Text-fig. 10, 11). The H6 negative peak above the inferred Michel Dean Event of the $\delta^{13}\text{C}_{\text{TOM}}$ curves, is correlated with the Haven Brow Isotope Event (Jarvis *et al.* 2006), based on the long-term trend of the $\delta^{13}\text{C}$ fluctuations. The H7 positive peak, below the occurrence of the Santonian ammonoid *Texanites (Plesiotexanites) kaswasakii* (Kawada), is the largest excursion in the lower part of the *I. amakusensis* Interval Zone, thus the $\delta^{13}\text{C}_{\text{TOM}}$ values decrease above this horizon. Because of this long-term trend, the H7 positive peak is correlated with the Horseshoe Bay Isotope Event (Jarvis *et al.* 2006).

The $\delta^{13}\text{C}_{\text{TOM}}$ curve in the upper part of the *I. amakusensis* Interval Zone is characterised by a negative peak (H8) and two positive peaks (H9 and H10). The $\delta^{13}\text{C}_{\text{carb}}$ profile displays a positive shift with short-term fluctuations through the Middle Santonian to the Santonian/Campanian boundary (Jarvis *et al.* 2006, Voigt *et al.* 2010). This long-term trend is similar to that of the $\delta^{13}\text{C}_{\text{TOM}}$ curve. Based on the long-term trend, the H8 negative peak is correlated with the Buckle Isotope Event (Jarvis *et al.* 2006), and the H9 positive peak with the Hawks Brow Isotope Event (Jarvis *et al.* 2006) (Text-fig. 10, 11). Jarvis *et al.* (2002) defined the Santonian/Campanian Boundary Event as a positive excursion at the Santonian/Campanian boundary. The $\delta^{13}\text{C}_{\text{carb}}$ values then decline through the Lower Cam-

panian, with small fluctuations (Jarvis *et al.* 2002, Voigt *et al.* 2010). This trend is recognised in the $\delta^{13}\text{C}_{\text{TOM}}$ curve of the Yezo Group, and the H10, the second significant positive peak, is correlated with the Santonian/Campanian Boundary Event (SCBE) (Text-fig. 10, 11). Voigt *et al.* (2010) demonstrated that the SCBE in the Lägerdorf-Kronsmoor-Hemmoor succession in northern Germany comprises a negative trough between two positive peaks (Text-fig. 10) and suggested that the stratigraphic interval at the Santonian/Campanian boundary was therefore condensed in the English Chalk. The $\delta^{13}\text{C}_{\text{TOM}}$ fluctuation pattern of the SCBE of the Yezo Group is similar to the SCBE $\delta^{13}\text{C}_{\text{carb}}$ fluctuations of the Lägerdorf-Kronsmoor-Hemmoor succession in northern Germany (Text-fig. 10). Moriya *et al.* (2001) reported the occurrence of the Lower Campanian planktonic foraminifer *Contusotruncana patelliformis* (Gandolfi) just above the UHs1 key bed, which is ~160 m above the Santonian/Campanian Boundary Event in the Haboro area and supports the chemostratigraphic correlation. Although the *I. amakusensis* Zone was hitherto correlated with the Santonian by Toshimitsu *et al.* (1995), the *I. amakusensis* Interval Zone actually correlates with the Middle/Upper Coniacian to the lower Lower Campanian (Text-fig. 10, 11).

The $\delta^{13}\text{C}_{\text{TOM}}$ profile in the *P. japonicus* Interval Zone is characterised by a negative peak (H11) and two positive peaks (H12 and H13). These peaks might be interpreted to correlate with the small fluctuations of the Lower Campanian $\delta^{13}\text{C}_{\text{carb}}$ profile (Jarvis *et al.* 2002, Voigt *et al.* 2010). However, the biostratigraphic correlations are not established above the Santonian/Campanian Boundary Event and the shape of the carbon isotope curves is different between Hokkaido and Europe. Although the *P. japonicus* zone was correlated with the basal Campanian to the lower Campanian by Toshimitsu (1988) and Toshimitsu *et al.* (1995), the *P. japonicus* Interval Zone is correlated with the upper Lower Campanian in this study (Text-fig. 10, 11).

Takashima *et al.* (2010) reported the correlation of the carbon isotope events in the Cenomanian–Campanian succession of the Kotanbetsu areas of Hokkaido; the correlations between their $\delta^{13}\text{C}$ profiles do not differ from those in this study (Text-fig. 10). However, their reported position of the lowest occurrence of *I. amakusensis* does differ significantly from ours.

Text-fig. 11. Correlation of the stratigraphic distributions of inoceramid ranges in the Haboro and Obira areas, the $\delta^{13}\text{C}_{\text{TOM}}$ curve in Japan (this study; Hasegawa and Saito 1993; Uramoto *et al.* 2007, 2009) and the reference $\delta^{13}\text{C}_{\text{carb}}$ curve of the English Chalk (Jarvis *et al.* 2002, 2006). Correlations of the carbon isotope fluctuations are indicated by grey bands and dashed lines. The stage boundaries are represented by the grey lines and grey dashed line. Macrofossil data after Tanabe *et al.* (1977), Matsumoto *et al.* (1981), Sekine *et al.* (1985), Toshimitsu (1985, 1988), Asai and Hirano (1990), Moriya and Hirano (2001), Moriya *et al.* (2001), Okamoto *et al.* (2003), Funaki and Hirano (2004), Oizumi *et al.* (2005) and this study. Inoceramid biozones after Funaki and Hirano (2004) and this study. Abbreviations: *I. v.*, *Inoceramus virgatus*; *A. nipponicus*, *Actinoceramus sp. ex gr. nipponicus*; *I. k.*, *Inoceramus kamuy*; *I. h.*, *Inoceramus hobetsensis*; *I. t.*, *Inoceramus teshioensis*; *I. u.*, *Inoceramus uwajimensis*; *Cr. m.*, *Cremonoceramus mihoensis*; *I. amakusensis.*, *Inoceramus amakusensis*; *P. japonicus*, *Platyceramus japonicus*; Alb., Albian; Co., Coniacian

Takashima *et al.* (2010) examined only a single section for the inoceramid biostratigraphy, based on records by Wani and Hirano (2000). The interpretation of the lowest occurrence of *I. amakusensis* differs because of the different correlations of the columnar sections between Wani and Hirano (2000) and Takashima *et al.* (2010) in the Kotanbetsu area and, moreover, because the identification of *I. amakusensis* is not correct (Hirano *et al.* 2011). The inoceramid biostratigraphy used in this study is a comprehensive compilation of our results since 1977 (Text-fig. 5) in both the Haboro and Obira areas and thus provides more reliable data.

Age of the occurrence of the inoceramids

The stratigraphic ranges of the inoceramids were studied by Nagao and Matsumoto (1939, 1940) for the first time, and summarised by Toshimitsu *et al.* (1995), Noda and Matsumoto (1998) and Takahashi (2005). However, the *I. uwajimensis* Interval Zone, *Cr. mihoensis* Interval Zone, *I. amakusensis* Interval Zone and *P. japonicus* Interval Zone are correlated herein with the uppermost Turonian, the Lower to Middle Coniacian, Middle/Upper Coniacian to lower Lower Campanian, and upper Lower Campanian, respectively, based on the chemostratigraphic correlations discussed above. Accordingly, the chronostratigraphic ages of the inoceramid zonal indices defined by Toshimitsu *et al.* (1995) are revised significantly. In this section, we describe the stratigraphic ranges of the inoceramids in detail.

The Middle/Upper Turonian boundary was proposed as the horizon of the lowest occurrence of the ammonoid *Romaniceras deverianum* (d'Orbigny) in the Tethyan biotic realm and as the horizon of the lowest occurrence of the ammonoid *Subprionocyclus neptuni* in the Boreal regions (Bengtson 1996). Subsequently, Wiese and Kaplan (2001) proposed as candidate GSSP for the Middle/Upper Turonian boundary the Lengerich quarry section in the Münster Basin of northern Germany and indicated that the horizon of the lowest occurrence of *Subprionocyclus neptuni* and *Inoceramus perplexus* Whitfield was useful for correlation. The occurrence of *Subprionocyclus cf. neptuni* was reported by Tanabe *et al.* (1977) in the *I. hobetsensis*-*I. teshioensis* Concurrent-range Zone in the Obira area of Hokkaido. Funaki and Hirano (2004) correlated this zone with the Middle/Upper Turonian boundary transition, and the *I. teshioensis* Partial-range Zone with the Upper Turonian. In the Obira area, the occurrence of *I. pedalionoides* is in the *I. teshioensis* Partial-range Zone, and the highest occurrence of this species is in the uppermost part of the *I. uwajimensis* Interval Zone. Consequently, *I. pedalionoides* is the Late Turonian species. Takahashi and

Mitsugi (2002) suggested that the range of *I. pedalionoides* overlapped with that of *I. hobetsensis* in the Teshionakagawa area, northern Hokkaido, and indicated the possibility that the lowest occurrence of *I. pedalionoides* was correlated with the Middle Turonian. On the basis of this correlation, *I. pedalionoides* can possibly range from the Middle Turonian to the Upper Turonian. *Mytiloides incertus* occurs together with *I. tenuistriatus* and *I. teshioensis* (Matsumoto and Noda 1983; Noda and Matsumoto 1998), and this species occurs in Upper Turonian strata worldwide (e.g., Matsumoto and Noda, 1983; Noda 1984; Noda and Matsumoto 1998; Dhondt 1992; Walaszczyk and Cobban 2000). Though the occurrence of *Mytiloides incertus* is rare in the study areas (Text-fig. 5, 6), it is mostly concurrent with *I. teshioensis* but not with *I. uwajimensis* in the Ikushunbetsu area, central Hokkaido (e.g., Noda and Matsumoto 1998). Thus, the range of *M. incertus* is included within the *I. teshioensis* Partial-range Zone. As previously mentioned, the *I. teshioensis* Partial-range Zone is correlated with the Upper Turonian (Funaki and Hirano 2004) and includes the Upper Turonian Bridgewick and Hitch Wood Isotope events. Therefore, the chronostratigraphic age of *M. incertus*, based on the $\delta^{13}\text{C}$ correlation, corresponds to the previous biostratigraphic interpretations (Matsumoto and Noda 1983; Noda 1984; Noda and Matsumoto 1998). The highest occurrence of *I. teshioensis* and the lowest occurrence of *I. uwajimensis* are between the Hitch Wood and Navigation Isotope events (Text-fig. 11). Thus, the lowest occurrence of *I. uwajimensis* is in the uppermost Turonian. This interpretation corresponds to the biostratigraphic correlation of Funaki and Hirano (2004). The occurrence of *Platyceramus szaszi* (Noda and Uchida) ranges from the *I. uwajimensis* Interval Zone to the *Cr. mihoensis* Interval Zone. This species was reported in the middle Coniacian by Noda and Uchida (1995). However, this study has shown that *P. szaszi* ranges from the uppermost Turonian to the Middle Coniacian because the highest occurrence of this species is below the inferred equivalent of the White Fall Isotope Event.

The base of the Coniacian is taken at the lowest occurrence of *Cremnoceramus deformis erectus* (Meek) (Kauffman *et al.* 1996; Walaszczyk and Wood 1998), and this horizon corresponds to the Navigation Isotope event (Jarvis *et al.* 2006). The Navigation Event is recognised in the lower part of the Haborogawa Formation by the correlation of the $\delta^{13}\text{C}_{\text{TOM}}$ fluctuations with the $\delta^{13}\text{C}_{\text{carb}}$ curve. The lowest occurrence of *Cr. mihoensis* is at this horizon. Although the occurrence of *Cr. mihoensis* was believed to indicate the upper Coniacian (e.g., Toshimitsu *et al.* 1995), the lowest occurrence of *Cr. mihoensis* marks the base of the Coniacian Stage.

The lowest occurrence of *Cordiceramus kawashitai* (Noda) is in the middle part of the *Cr. mihoensis* Interval Zone (Text-fig. 11). The lowest occurrence of *I. amakusensis* is below the horizon of the Kingsdown Isotope Event. The occurrence of *I. amakusensis* was correlated with the Santonian (Toshimitsu 1988; Toshimitsu *et al.* 1995). In this study, however, the lowest occurrence of *I. amakusensis* is in the Middle Coniacian. The occurrence of *P. mantelli* was correlated with the upper Coniacian through the Santonian in the conventional biostratigraphic scheme in the North Pacific province (Noda and Toshimitsu 1990). However, the lowest occurrence of this species is in the Middle Coniacian because this horizon is between the White Fall and Kingsdown Isotope events.

The base of the Santonian is marked by the lowest occurrence of *Cladoceramus undulatoplicatus* (Roemer) (Lamolda and Hancock 1996), which is associated with the Michel Dean Isotope Event (Jarvis *et al.* 2006). *I. amakusensis*, *P. mantelli* and *S. naumanni* occur in the Santonian succession, and the highest occurrence of these species is above the Santonian/Campanian Boundary Event.

The base of the Campanian is taken at the highest occurrence of the crinoid *Marsupites testudinarius* (von Schlotheim) (Hancock and Gale 1996), which corresponds to the Santonian/Campanian Boundary Isotope Event (Jarvis *et al.* 2002, 2006). The highest occurrence of *I. amakusensis* and *P. mantelli* is just above the horizon of the Santonian/Campanian Boundary Event, and the highest occurrence of these species is correlated with the lowermost Campanian. *P. ezoensis* ranges from the uppermost part of the *I. amakusensis* Interval Zone to the *P. japonicus* Interval Zone, which is correlative with the lower Campanian, but not with the basal part of the stage (Text-fig. 11). The occurrence of *P. japonicus* is correlated with the upper Lower Campanian.

Takashima *et al.* (2010) correlated their bulk wood $\delta^{13}\text{C}$ curve with the $\delta^{13}\text{C}_{\text{carb}}$ record of the English Chalk reported by Jarvis *et al.* (2006). They correlated the *I. uwajimensis*, *I. amakusensis* and *P. japonicus* zones with the uppermost Turonian, basal Coniacian to basal Campanian and upper Lower Campanian respectively. They investigated the high-resolution chemostratigraphy of the sections along the Kotanbetsu River, which is located between the Haboro and Obira areas. Takashima *et al.* (2010) used the inoceramid records reported by Wani and Hirano (2000); however records from a single section in one area would be inadequate to enable revision of the Japanese inoceramid biozonal scheme. The inoceramid biostratigraphy of the Yezo Group is herein revised significantly, at least in northwestern Hokkaido. Further studies are needed to improve the in-

oceramid biozonal scheme in the North Pacific biogeographic province.

Implications of the revised inoceramid biostratigraphy

The uppermost Turonian of the Euramerican region is characterised by the disappearance of the *Mytiloides* group and the lowest occurrence of *Cremnoceramus* (Walaszczyk and Wood 1998; Walaszczyk and Cobban 2000). The period from the Middle Coniacian to the Santonian of the United States Western Interior and Europe represents the highest taxonomic and morphological diversity in inoceramids (Walaszczyk and Cobban 2006). Meanwhile, Takahashi (2005) showed the diversity changes in the Japanese inoceramids in the context of the previous biozonal scheme, but did not refer to the differences in these changes between Japan and Euramerica. Thus, it is important to discuss the differences in the diversity changes in inoceramids between Japan and Euramerica using the revised inoceramid biozones and chronostratigraphic ages for the Coniacian through Santonian interval, with the aim of evaluating the timing of the originations and the extinctions between the inoceramid evolutionary patterns and the environmental factors in each biogeographic region for further study.

In Europe and the Western Interior of the United States, the Turonian/Coniacian, Lower/Middle Coniacian, Middle/Upper Coniacian and Coniacian/Santonian boundaries are generally determined by the lowest occurrence of the age-diagnostic inoceramid species, and these boundaries correspond to changes in the generic composition of the inoceramid assemblages (e.g., Walaszczyk and Wood 1998; Walaszczyk and Cobban 2000; Walaszczyk and Cobban 2006). The base of the Coniacian is taken at the lowest occurrence of *Cremnoceramus deformis erectus* (Kauffman *et al.* 1996; Walaszczyk and Wood 1998; Walaszczyk and Cobban 2000). The Lower/Middle Coniacian boundary is taken at the lowest occurrence of *Volviceramus koeneni* (G. Müller) (Kauffman *et al.* 1996) and the Middle/Upper Coniacian boundary at the lowest occurrence of *Magadiceramus subquadratus* (Schlüter) (Kauffman *et al.* 1996). The base of the Santonian is taken at the lowest occurrence of *Cladoceramus undulatoplicatus* (Roemer) (Lamolda and Hancock 1996). These genera, including the age-diagnostic species, characterise each stage or substage: *Cremnoceramus* indicates the Lower Coniacian, *Volviceramus* the Middle Coniacian, *Magadiceramus* the Upper Coniacian, and *Cladoceramus* the Santonian in the Euramerican region (Walaszczyk and Wood 1998; Walaszczyk and Cobban 2000; Walaszczyk and Cobban 2006). Moreover, the highest occurrence of *Cladoceramus undulatoplicatus* has been suggested as a

boundaries in Hokkaido, based on the chemostratigraphic correlations (Text-fig. 12). Takahashi (2005) reported high extinction rates at the Turonian/Coniacian boundary (75.0%) and at the Lower/Middle Coniacian boundary (70.0%). Takahashi (2005) also indicated that the generic composition of the inoceramid assemblage changed drastically at the Turonian/Coniacian boundary. Nevertheless, the previous Turonian/Coniacian and the Lower/Middle Coniacian boundaries are correlated with the uppermost Turonian by the chemostratigraphic correlations in this study. Therefore, the low extinction rates, constant origination rates and similar generic compositions were shown from the Turonian/Coniacian boundary (Middle/Upper Coniacian boundary of Takahashi 2005) to the Santonian/Campanian boundary (Takahashi 2005). The results of this study reflect the trend of inoceramid diversity changes in Japan (Takahashi 2005), and the timing of originations and extinctions of inoceramids does not correspond to the stage or substage boundaries.

It is reasonable to suggest that the timing of originations and extinctions of inoceramids in Japan is different from those of Europe and North America. Because the Santonian Stage in Japan could not be subdivided by using the inoceramid biozones (Text-fig. 12) and has not been subdivided into substages, we do not discuss the difference of the changes in the generic composition above the Middle Santonian between the North Pacific biotic province and the Euramerican biogeographic region. Therefore, inoceramids belonging to the North Pacific biotic province would have been controlled by different bioevents from those in the Euramerican region, at least in the interval from the Early Coniacian to Early Santonian.

CONCLUSIONS

We presented high-resolution carbon isotope records of terrestrial organic matter for the Yezo Group in the Haboro and Obira areas of northwestern Hokkaido, Japan. The integrated $\delta^{13}\text{C}_{\text{TOM}}$ curve correlates with the $\delta^{13}\text{C}_{\text{carb}}$ record in England and Germany for the Upper Turonian–Lower Campanian interval. Based on the chemostratigraphic correlations, we recognised 11 of the isotope events identified in the English Chalk by Jarvis *et al.* (2006): the Bridgewick Event, the Hitch Wood Event, the Navigation Event, the White Fall Event, the Kingsdown Event, the Michel Dean Event, the Haven Brow Event, the Horseshoe Bay Event, the Buckle Event, the Hawks Brow Event and the Santonian/Campanian Boundary Event. Based on the recognition of these isotopic events, we revised the chronostratigraphic ages of the inoceramid biozones of the Yezo Group.

- 1) The *Inoceramus uwajimensis* Interval Zone is defined as the stratigraphic interval from the lowest occurrence of *I. uwajimensis* to that of *Cremonoceramus mihoensis*. The age of this zone is latest Late Turonian.
- 2) The *Cremonoceramus mihoensis* Interval Zone is defined as the stratigraphic interval from the lowest occurrence of *Cr. mihoensis* to that of *Inoceramus amakusensis*. The age of this zone is Early to Middle Coniacian.
- 3) The *Inoceramus amakusensis* Interval Zone is defined as the stratigraphic interval from the lowest occurrence of *I. amakusensis* to that of *Platyceramus japonicus*. The age of this zone is the Middle/Late Coniacian to early Early Campanian.
- 4) The *Platyceramus japonicus* Interval Zone is defined as the stratigraphic interval from the lowest occurrence of *P. japonicus* to that of *Sphenoceramus schmidtii*. The age of this zone is late Early Campanian. This correlation suggests that the timing of the inoceramid originations and/or extinctions differs that of the stage and substage boundaries in the interval from the Lower Coniacian to the Santonian. The timing of the diversity changes in the North Pacific inoceramids is inconsistent with those in the Euramerican region for this period.

Acknowledgments

We gratefully thank Dr. A. Takahashi for his critical reading, Dr. K. Moriya for his helpful comments on the manuscript, and Dr. G. Uramoto, Mr. K. Seike and Mr. B. Honda for their suggestions and support throughout the fieldwork. We express gratitude to Dr. A. Waseda for analytical guidance, and Mr. Y. Kajiwara, Mr. Nishita and Ms. M. Aoyama of JAPEX Research Center for their analytical support. We wish to thank Prof. S. Voigt for her constructive comments. We are also grateful to Prof. K.-A. Tröger, Mr. C.J. Wood and an anonymous reviewer for comments which helped to improve our manuscript.

Messrs. M. Obayashi, Y. Kojima, H. Koyasu and S. Miyata helped the first author at Waseda University. This study is financially supported by the Grant-in-Aid for Scientific Research (B) of JSPS (no. 19340157; 2007-2009 for HH) and the Grant-in-Aid for Special Research of Waseda Univ. (2010A-022 for HH).

REFERENCES

- Ando, H. 2003. Stratigraphic correlation of Upper Cretaceous to Paleocene forearc basin sediments in Northeast Japan: Cyclic sedimentation and basin evolution. *Journal of Asian Earth Sciences*, **21**, 921–935.

- Ando, A. and Kakegawa, T. 2007. Carbon isotope record of terrestrial organic matter and occurrence of planktonic foraminifera from the Albian Stage of Hokkaido, Japan: ocean-atmosphere $\delta^{13}\text{C}$ trends and chronostratigraphic implications. *Palaios*, **22**, 417–432.
- Ando, A., Kakegawa, T., Takashima, R. and Saito, T. 2002. New perspective on Aptian carbon isotope stratigraphy: Data from $\delta^{13}\text{C}$ records of terrestrial organic matter. *Geology*, **30**, 227–230.
- Ando, A., Kakegawa, T., Takashima, R. and Saito, T. 2003. Stratigraphic carbon isotope fluctuations of detrital woody materials during the Aptian Stage in Hokkaido, Japan: Comprehensive $\delta^{13}\text{C}$ data from four sections of the Ashibetsu area. *Journal of Asian Earth Sciences*, **21**, 835–847.
- Asai, A. and Hirano, H. 1990. Stratigraphy of the Upper Cretaceous in the Obira area, northwestern Hokkaido. *Gakujutsu Kenkyu, School of Education, Waseda University, Series Biology and Geology*, **39**, 37–50.
- Bengtson, P. 1996. The Turonian stage and substage boundaries. *Bulletin de l'Institut Royal des Sciences Naturelles de Belgique, Science de la Terre*, **66** (Supplement), 69–79.
- Dhondt, A.V. 1992. Cretaceous inoceramid biogeography: review. *Palaeogeography, Palaeoclimatology, Palaeoecology*, **92**, 217–232.
- Diebold, F., Bengtson, P., Lees, J. and Walaszczyk, I. 2010. ammonite, inoceramid and nannofossil biostratigraphy across the Turonian–Coniacian boundary in the Aquitaine and Vocontian basins (France) and Diego Basin (Madagascar). 8th International Symposium Cephalopods – Present and Past, Dijon, France, August 30th to September 3rd, 2010, abstract Volume.
- Erbacher, J., Thurow, J. and Littke, R. 1996. Evolution patterns of radiolarian and organic matter variations: A new approach to identify sea-level changes in mid-Cretaceous pelagic environments. *Geology*, **24**, 499–502.
- Funaki, H. and Hirano, H. 2004. Cretaceous stratigraphy in the northeastern part of the Obira area, Hokkaido, Japan. *Bulletin of the Mikasa City Museum* **8**, 17–35. [In Japanese with English abstract]
- Gale, A.S. 1996. Turonian correlation and sequence stratigraphy of the Chalk in southern England. In: S.P. Hesselbo and D.N. Parkinson (Eds), *Sequence Stratigraphy in British Geology*. Geological Society of London, Special Publication, **103**, 177–195.
- Gale, A.S., Hancock, J.M., Kennedy, W.J., Petrizzo, M.R., Lees, J.A., Walaszczyk, I. and Wray, D.S. 2008. An integrated study (geochemistry, stable oxygen and carbon isotopes, nannofossils, planktonic foraminifera, inoceramid bivalves, ammonites and crinoids) of the Waxahachie Dam Spillway section, north Texas: a possible boundary stratotype for the base of the Campanian Stage. *Cretaceous Research*, **29**, 131–167.
- Hancock, J.M. and Gale, A.S. 1996. The Campanian Stage. *Bulletin de l'Institut Royal des Sciences Naturelles de Belgique, Science de la Terre*, **66** (Supplement), 103–109.
- Hasegawa, T. 1992. Positive excursion of isotopic ratio of organic carbon near the Cenomanian/Turonian boundary in the Upper Cretaceous Yezo Group. *Fossils (Palaeontological Society of Japan)*, **53**, 33–37. [In Japanese]
- Hasegawa, T. 1997. Cenomanian-Turonian carbon isotope events recorded in terrestrial organic matter from northern Japan. *Palaeogeography, Palaeoclimatology, Palaeoecology*, **130**, 251–273.
- Hasegawa, T. and Hatsugai, T. 2000. Carbon-isotope stratigraphy and its chronostratigraphic significance for the Cretaceous Yezo Group, Kotanbetsu area, Hokkaido, Japan. *Paleontological Research*, **4**, 95–106.
- Hasegawa, T., Pratt, L.M., Maeda, H., Shigeta, Y., Okamoto, T., Kase, T. and Uemura, K. 2003. Upper Cretaceous stable carbon isotope stratigraphy of terrestrial organic matter from Sakhalin, Russian Far East: a proxy for the isotopic composition of paleoatmospheric CO_2 . *Palaeogeography, Palaeoclimatology, Palaeoecology*, **189**, 97–115.
- Hasegawa, T. and Saito, T. 1993. Global synchronicity of a positive carbon isotope excursion at the Cenomanian/Turonian boundary: Validation by calcareous microfossil biostratigraphy of the Yezo Group, Hokkaido, Japan. *Island Arc*, **3**, 181–191.
- Hirano, H. and Fukuju, T. 1997. Lower Cretaceous oceanic anoxic event in the Lower Yezo Group, Hokkaido, Japan. *Journal of the Geological Society of the Philippines*, **52**, 173–182.
- Hirano, H., Toshimitsu, S., Honda, B. and Hayakawa, T. 2011. Cretaceous biostratigraphy—Efforts toward integration. In: Kondo, M., Iwai, M., Murayama, M. and Nara, M. (Eds), *Abstracts with Programs, the 160th Regular Meeting. The Palaeontological Society of Japan*, p. 7. Kochi.
- Hunt, J.M. 1996. *Petroleum Geochemistry and Geology*, pp. 1–743. 2nd ed. W.H. Freeman Company; New York.
- Iba, Y. and Sano, S. 2007. Mid-Cretaceous step-wise demise of the carbonate platform biota in the Northwest Pacific and establishment of the North Pacific biotic province. *Palaeogeography, Palaeoclimatology, Palaeoecology*, **245**, 462–482.
- Igi, S., Tanaka, K., Hata, M. and Saito, H. 1958. Explanatory text of the geological map of Japan, scale 1:50000, Horokanai, pp. 1–64. Geological Survey of Japan; Kawasaki. [In Japanese with English abstract]
- Jarvis, I., Gale, A.S., Jenkyns, H.C. and Pearce, M.A. 2006. Secular variation in Late Cretaceous carbon isotopes: a new $\delta^{13}\text{C}$ carbonate reference curve for the Cenomanian–Campanian (99.6–70.6 Ma). *Geological Magazine*, **143**, 561–608.

- Jarvis, I., Mabrouk, A., Moody, R.T.J. and De Cabrera, S.C. 2002. Late Cretaceous (Campanian) carbon isotope events, sea-level change and correlation of the Tethyan and Boreal realms. *Palaeogeography, Palaeoclimatology, Palaeoecology*, **188**, 215–248.
- Jenkyns, H.C., Gale, A.S. and Corfeld, R.M. 1994. Carbon and oxygen-isotope stratigraphy of the English Chalk and Italian Scaglia and its palaeoclimatic significance. *Geological Magazine*, **131**, 1–34.
- Kauffman, E.G., Kennedy, W.J. and Wood, C.J. 1996. The Coniacian stage and substage boundaries. *Bulletin de l'Institut Royal des Sciences Naturelles de Belgique, Science de la Terre*, **66** (Supplement), 81–94.
- Lamolda, M.A. and Hancock, J.M. 1996. The Santonian Stage and substages. *Bulletin de l'Institut Royal des Sciences Naturelles de Belgique, Science de la Terre*, **66** (Supplement), 95–102.
- Matsumoto, T. 1959. Zonation of the Upper Cretaceous in Japan. *Memoirs of the Faculty of Science, Kyushu University, Series D, Geology*, **9**, 55–93.
- Matsumoto, T., Muramoto, K., Hirano, H. and Takahashi, T. 1981. Some Coniacian ammonites from Hokkaido (Studies of the Cretaceous ammonites from Hokkaido-XL). *Transactions and Proceedings of the Palaeontological Society of Japan, New Series*, **121**, 51–73.
- Matsumoto, T. and Noda, M. 1983. Restudy of *Inoceramus incertus* Jimbo with special reference to its biostratigraphic implications. *Proceedings of Japanese Academy of Science B*, **59**, 109–112.
- Moriya, K. and Hirano, H. 2001. Cretaceous stratigraphy in the Chikubetsu area, Hokkaido. *Journal of the Geological Society of Japan*, **107**, 199–214. [In Japanese with English abstract]
- Moriya, K., Nishi, H. and Tanabe, K. 2001. Age calibration of megafossil biochronology based on Early Campanian planktonic foraminifera from Hokkaido, Japan. *Paleontological Research*, **5**, 277–282.
- Nagao, T. and Matsumoto, T. 1939. A monograph of the Cretaceous *Inoceramus* of Japan. Part. 1. *Journal of the Faculty of Science, Hokkaido Imperial University Series* **4**, **4**, 241–299.
- Nagao, T. and Matsumoto, T. 1940. A monograph of the Cretaceous *Inoceramus* of Japan. Part. 2. *Journal of the Faculty of Science, Hokkaido Imperial University Series* **4**, **6**, 1–64.
- Nishi, H., Takashima, R., Hatsugai, T., Saito, T., Moriya, K., Ennyu, A. and Sakai, T. 2003. Planktonic foraminiferal zonation in the Cretaceous Yezo Group, Central Hokkaido, Japan. *Journal of Asian Earth Sciences*, **21**, 867–886.
- Noda, M. 1984. Notes on *Mytiloides incertus* (Cretaceous *Bivalvia*) from the Upper Turonian of the Pombets area, central Hokkaido. *Transactions and Proceedings of the Palaeontological Society of Japan, New Series*, **136**, 455–473.
- Noda, M. and Matsumoto, T. 1998. Palaeontology and stratigraphy of the inoceramid species from the mid-Turonian through upper Middle Coniacian in Japan. *Acta Geologica Polonica*, **48**, 435–482.
- Noda, M. and Toshimitsu, S. 1990. Notes on a Cretaceous bivalve *Inoceramus (Platyceramus) mantelli* De Mercey from Japan. *Transactions and Proceedings of the Palaeontological Society of Japan, New Series*, **158**, 485–512.
- Noda, M. and Uchida, S. 1995. *Inoceramus (Platyceramus) szaszi* sp. nov. (Bivalvia) from the Coniacian (Cretaceous) of Hokkaido, Japan. *Transactions and Proceedings of the Palaeontological Society of Japan, New Series*, **178**, 142–153.
- Ogg, J.G., Agterberg, F.P. and Gradstein, F.M. 2004. The Cretaceous Period. In: F.M. Gradstein, J.G. Ogg and A.G. Smith (Eds), *A Geologic Time Scale 2004*, 344–383.
- Oizumi, M., Kurihara, K., Funaki, H. and Hirano, H. 2005. Upper Cretaceous stratigraphy in the Obira area, Hokkaido, Japan. *Bulletin of the Mikasa City Museum*, **9**, 11–26. [In Japanese with English abstract]
- Okada, H. 1982. Geologic evolution of Hokkaido, Japan: an example of collision orogenesis. *Proceedings of Geologist's Association*, **93**, 201–212.
- Okamoto, T., Matsunaga, T. and Okada, M. 2003. Restudy of the Upper Cretaceous stratigraphy in the Haboro area, northwestern Hokkaido. *Journal of the Geological Society of Japan*, **109**, 363–382.
- Scholle, P.A. and Arthur, M.A. 1980. Carbon Isotope Fluctuation in Cretaceous Pelagic Limestones: Potential Stratigraphic and Petroleum Exploration Tool. *The American Association of Petroleum Geologists Bulletin*, **64**, 67–87.
- Sekine, H., Takagi, A. and Hirano, H. 1985. Biostratigraphical study of the Upper Cretaceous of the north-east part of the Obira area, Hokkaido. *Fossils (Palaeontological Society of Japan)*, **38**, 1–15. [In Japanese with English abstract]
- Stoll, H.M. and Schrag, D.P. 2000. High-resolution stable isotope records from the Upper Cretaceous rocks of Italy and Spain: Glacial episodes in a greenhouse planet? *Geological Society of America Bulletin* **112**, 308–319.
- Tröger, K.-A. 1967. Zur Paläontologie, Biostratigraphie und faziellen Ausbildung der unteren Oberkreide (Cenoman bis Turon). Teil 1. Paläontologie und Biostratigraphie der Inoceramen des Cenomans bis Turons Mitteleuropas. *Abhandlungen des Staatlichen Museums für Mineralogie und Geologie zu Dresden*, **12**, 13–208. Dresden.
- Takahashi, A. 2005. Diversity changes in Cretaceous inoceramid bivalves of Japan. *Paleontological Research*, **9**, 217–232.
- Takahashi, A. and Mitsugi, T. 2002. Fossils from the channel-fill deposits of the Upper Cretaceous Saku Formation in

- the Teshionakagawa area, Hokkaido, Japan, and their significance. *Journal of the Geological Society of Japan*, **108**, 281–190. [In Japanese with English abstract]
- Takashima, R., Kawabe, F., Nishi, H., Moriya, K., Wani, R. and Ando, H. 2004. Geology and stratigraphy of forearc basin sediments in Hokkaido, Japan: Cretaceous environmental events on the north-west Pacific margin. *Cretaceous Research*, **25**, 365–390.
- Takashima, R., Nishi, H., Yamanaka, T., Hayashi, K., Waseda, A., Obuse, A., Tomosugi, T., Deguchi, N. and Mochizuki, S. 2010. High-resolution terrestrial carbon isotope and planktic foraminiferal records of the Upper Cenomanian to the Lower Campanian in the Northwest Pacific. *Earth and Planetary Science Letters*, **289**, 570–582.
- Tanabe, K., Hirano, H., Matsumoto, T. and Miyata, Y. 1977. Stratigraphy of the Upper Cretaceous deposits in the Obira area, northwestern Hokkaido. *Memoirs of the Faculty of Science, Kyushu University, Series D, Geology*, **12**, 181–202. [In Japanese with English abstract]
- Tanaka, K. 1963. A study on the Cretaceous sedimentation in Hokkaido, Japan. *Report of Geological Survey of Japan*, **197**, 1–122.
- Toshimitsu, S. 1985. Biostratigraphy and depositional facies of the Cretaceous in the upper reaches of the Haboro River, Hokkaido. *Journal of the Geological Society of Japan*, **91**, 599–618. [In Japanese with English abstract]
- Toshimitsu, S. 1988. Biostratigraphy of the Upper Cretaceous Santonian Stage in northwestern Hokkaido. *Memoirs of the Faculty of Science, Kyushu University, Series D, Geology*, **26**, 125–192.
- Toshimitsu, S., Hasegawa, T. and Tsuchiya, K. 2007. Coniacian-Santonian Stratigraphy in Japan: a review. *Cretaceous Research*, **28**, 128–131.
- Toshimitsu, S., Maiya, S., Inoue, Y. and Takahashi, T. 1998. Integrated megafossil-foraminiferal biostratigraphy of the Santonian to lower Campanian (Upper Cretaceous) succession in northwestern Hokkaido, Japan. *Cretaceous Research*, **19**, 69–85.
- Toshimitsu, S., Matsumoto, T., Noda, M., Nishida, T. and Maiya, S. 1995. Towards an integrated mega-, micro-, and magneto-stratigraphy of the Upper Cretaceous in Japan. *Journal of the Geological Society of Japan*, **101**, 19–29. [In Japanese with English abstract]
- Tsuchiya, K., Hasegawa, T. and Pratt, L.M. 2003. Stratigraphic relationship between diagnostic carbon isotope profiles and inoceramid biozones from the Yezo Group, Hokkaido, Japan. *Journal of the Geological Society of Japan*, **109**, 30–40. [In Japanese with English abstract]
- Tsushima, K., Tanaka, K., Matsuno, K. and Yamaguchi, S. 1958. Explanatory text of the geological map of Japan, scale 1:50000, Tappu, pp. 1–74. Geological Survey of Japan; Kawasaki. [In Japanese with English abstract]
- Uramoto, G., Abe, Y. and Hirano, H. 2009. Carbon isotope fluctuations of terrestrial organic matter for the Upper Cretaceous (Cenomanian-Santonian) in the Obira area of Hokkaido, Japan. *Geological Magazine*, **146**, 761–774.
- Uramoto, G., Fujita, T., Takahashi, A. and Hirano, H. 2007. Cenomanian (Upper Cretaceous) carbon isotope stratigraphy of terrestrial organic matter for the Yezo Group, Hokkaido, Japan. *Island Arc*, **16**, 465–478.
- Voigt, S. 2000. Cenomanian-Turonian composite $\delta^{13}\text{C}$ curve for Western and Central Europe: the role of organic and inorganic carbon fluxes. *Palaeogeography, Palaeoclimatology, Palaeoecology*, **160**, 91–104.
- Voigt, S., Friedrich, O., Norris, R.D. and Schönfeld, J. 2010. Campanian-Maastrichtian carbon isotope stratigraphy: shelf-ocean correlation between the European shelf sea and the tropical Pacific Ocean. *Newsletters on Stratigraphy*, **44**, 57–72.
- Voigt, S. and Hilbrecht, H. 1997. Late Cretaceous carbon isotope stratigraphy in Europe: correlation and relations with sea level and sediment stability. *Palaeogeography, Palaeoclimatology, Palaeoecology*, **134**, 39–59.
- Walaszczyk, I. and Wood, C.J. 1998. Inoceramids and biostratigraphy at the Turonian/Coniacian boundary; based on the Salzgitter-Salder Quarry, Lower Saxony, Germany, and the Słupia Nadbrzeżna section, Central Poland. *Acta Geologica Polonica*, **48**, 395–434.
- Walaszczyk, I. and Cobban, W.A. 2000. Inoceramid faunas and biostratigraphy of the Upper Turonian-Lower Coniacian of the Western Interior of the United States. *Special Papers in Palaeontology*, **64**, 1–118.
- Walaszczyk, I. and Cobban, W.A. 2006. Palaeontology and biostratigraphy of the Middle-Upper Coniacian and Santonian inoceramids of the US Western Interior. *Acta Geologica Polonica*, **56**, 241–348.
- Wani, R. and Hirano, H. 2000. Upper Cretaceous biostratigraphy in the Kotanbetsu area, northwestern Hokkaido. *Journal of the Geological Society of Japan*, **106**, 171–188. [In Japanese with English abstract]
- Whiticar, M.J. 1996. Stable isotope geochemistry of coals, humic kerogens and related natural gas. *International Journal of Coal Geology*, **32**, 191–215.
- Wiese, F. and Kaplan, U. 2001. The potential of the Lengerich section (Munster Basin, northern Germany) as a possible candidate Global boundary Stratotype Section and Point (GSSP) for the Middle/Upper Turonian boundary. *Cretaceous Research*, **22**, 549–563.
- Wood, C.J., Ernst, G. and Rasemann, G. 1984. The Turonian-Coniacian stage boundary in Lower Saxony (Germany) and adjacent areas: the Salzgitter-Salder Quarry as a proposed international standard section. *Bulletin of the Geological Society of Denmark*, **33**, 225–238.
- Wood, C.J., Walaszczyk, I., Mortimore, R.N. and Woods, M.A. 2004. New observations

on the inoceramid biostratigraphy of the higher part of the Upper Turonian and the Turonian – Coniacian boundary transition in Poland, Germany and the UK. *Acta Geologica Polonica*, **54**, 541–549.

Yamaguchi, S. and Matsuno, K. 1963. Explanatory text of the geological map of Japan, scale 1:50000, Sankei, pp. 1–50. Geological Survey of Japan; Kawasaki. [In Japanese with English abstract]

Manuscript submitted: 15th January 2012

Revised version accepted: 15th April 2013